Climate Dynamics

Responses of European precipitation distributions and regimes to different blocking locations

--Manuscript Draft--

Manuscript Number:	CLDY-D-15-00670R1
Full Title:	Responses of European precipitation distributions and regimes to different blocking locations
Article Type:	Original Article
Keywords:	atmospheric blocking; precipitation; Europe; Weather regimes; PDF
Corresponding Author:	Pedro Miguel Sousa IDL - University of Lisbon PORTUGAL
Corresponding Author Secondary Information:	
Corresponding Author's Institution:	IDL - University of Lisbon
Corresponding Author's Secondary Institution:	
First Author:	Pedro Miguel Sousa
First Author Secondary Information:	
Order of Authors:	Pedro Miguel Sousa
	Ricardo M Trigo
	David Barriopedro
	Pedro M M Soares
	Alexandre M Ramos
	Margarida L R Liberato
Order of Authors Secondary Information:	
Funding Information:	Fundação para a Ciência e a Tecnologia (SFRH/BD/84395/2012) — Dr. Pedro Miguel Sousa
	Fundação para a Ciência e a Tecnologia (PT) (DFRH/SFRH/BPD/84328/2012) — Dr Alexandre M Ramos
	Fundação para a Ciência e a Tecnologia (PTDC/GEOMET/7078/2014) — Dr Pedro M M Soares
Abstract:	In this work we performed an analysis on the impacts of blocking episodes on seasonal and annual European precipitation and the associated physical mechanisms. Distinct domains were considered in detail taking into account different blocking center positions spanning between the Atlantic and western Russia. Significant positive precipitation anomalies are found for southernmost areas while generalized negative anomalies (up to 75 % in some areas) occur in large areas of central and northern Europe. This dipole of anomalies is reversed when compared to that observed during episodes of strong zonal flow conditions. We illustrate that the location of the maximum precipitation anomalies follows quite well the longitudinal positioning of the blocking centers and discuss regional and seasonal differences in the precipitation responses. To better understand the precipitation anomalies, we explore the blocking influence on cyclonic activity. The results indicate a split of the storm-tracks north and south of blocking systems, leading to an almost complete reduction of cyclonic centers in northern and central Europe and increases in southern areas, where cyclone frequency doubles during blocking episodes. However, the underlying processes conductive to the precipitation anomalies are distinct between northern and southern European regions, with a significant role of atmospheric instability in southern Europe,

	and moisture availability as the major driver at higher latitudes. This distinctive underlying process is coherent with the characteristic patterns of latent heat release from the ocean associated with blocked and strong zonal flow patterns. We also analyzed changes in the full range of the precipitation distribution of several sectors during blocked and zonal days. Results show that precipitation reductions in the areas under direct blocking influence are driven by a substantial drop in the frequency of moderate rainfall classes. Contrarily, southwards of blocking systems, frequency increases in moderate to extreme rainfall classes largely determine the precipitation anomaly in the accumulated totals. In this context, we show the close relationship between the more intrinsic torrential nature of Mediterranean precipitation regimes and the role of blocking systems in increasing the probability of extreme events.

Responses of European precipitation distributions and regimes to different blocking locations

Pedro M. Sousa[1], Ricardo M. Trigo[1], David Barriopedro[2, 3] Pedro M. M. Soares[1], Alexandre M. Ramos[1], Margarida L.R. Liberato [1,4]

[1]University of Lisbon, CGUL, IDL, Lisbon, Portugal

[2]Departamento de Física de la Tierra II, Facultad de Ciencias Físicas, Universidad Complutense de Madrid, Spain

[3]Instituto de Geociencias (IGEO), CSIC-UCM, Madrid, Spain

[4] Escola de Ciências e Tecnologia, Universidade de Trás-os-Montes e Alto Douro, UTAD, 5000-801 Vila Real, Portugal

Abstract

In this work we performed an analysis on the impacts of blocking episodes on seasonal and annual European precipitation and the associated physical mechanisms. Distinct domains were considered in detail taking into account different blocking center positions spanning between the Atlantic and western Russia. Significant positive precipitation anomalies are found for southernmost areas while generalized negative anomalies (up to 75 % in some areas) occur in large areas of central and northern Europe. This dipole of anomalies is reversed when compared to that observed during episodes of strong zonal flow conditions. We illustrate that the location of the maximum precipitation anomalies follows quite well the longitudinal positioning of the blocking centers and discuss regional and seasonal differences in the precipitation responses.

To better understand the precipitation anomalies, we explore the blocking influence on cyclonic activity. The results indicate a split of the storm-tracks north and south of blocking systems, leading to an almost complete reduction of cyclonic centers in northern and central Europe and increases in southern areas, where cyclone frequency doubles during blocking episodes. However, the underlying processes conductive to the precipitation anomalies are distinct between northern and southern European regions, with a significant role of atmospheric instability in southern Europe, and moisture availability as the major driver at higher latitudes. This distinctive underlying process is coherent with the characteristic patterns of latent heat release from the ocean associated with blocked and strong zonal flow patterns.

We also analyzed changes in the full range of the precipitation distribution of several sectors during blocked and zonal days. Results show that precipitation reductions in the areas under direct blocking influence are driven by a substantial drop in the frequency of moderate rainfall classes. Contrarily, southwards of blocking systems, frequency increases in moderate to extreme rainfall classes largely determine the precipitation anomaly in the accumulated totals. In this context, we show the close relationship between the more intrinsic torrential nature of Mediterranean precipitation regimes and the role of blocking systems in increasing the probability of extreme events.

1. Introduction

Blocking systems wield a significant role on the atmospheric dynamics of mid-latitude regions, and their frequency and variability impinge on the climatology of large continental areas. As a result, these high latitude quasi-stationary anticyclones have been frequently studied throughout the last decades, regarding their climatology and characterization (e.g., Rex, 1950a,b; Treidl et al. 1981; Barriopedro et al. 2006, 2010a; Croci-Maspoli et al. 2007; Davini et al. 2012), their specific impacts (e.g., Trigo et al. 2004; Sillmann and Croci-Maspoli 2009a; Buehler et al. 2011; Barriopedro et al. 2011; Ruti et al. 2014; Sousa et al. 2015), as well as their representation in General Circulation Models (Barriopedro et al. 2010a,b, Matsueda et al. 2009; Scaife et al. 2010; Barnes et al. 2012; Vial and Osborn 2012: Anstey et al. 2013; Dunn-Sigouin and Son 2013; Masato et al. 2013). Previous studies have found that, over the Euro-Atlantic sector, the occurrence of winter blocking systems disrupts the dominant zonal circulation that affects the European continent, often leading to a reversal of this prevailing westerly flux. As a consequence, low-pressure systems travelling from the Atlantic towards Europe are diverted from their usual paths, resulting in a large decrease of rainfall for most of the European countries. An exception can be found for southernmost and northernmost sectors of Europe, which experience increased precipitation due to a bifurcation of the storm-track around the blocking high structure (Trigo et al. 2004; Nieto et al. 2007; Sousa et al. 2015).

It is worth mentioning the differences between a blocking pattern and a subtropical ridge (Barriopedro et al. 2010a) although sometimes they can induce similar anomalies in surface climate variables (García-Herrera et al. 2010). Some authors have shown that northward strengthening's of sub-tropical ridges in the Eastern Atlantic during the wet season have opposite precipitation responses in Western and Southern Europe to those associated with blocking (e.g. Santos et al. 2009, 2013). Such separation of phenomena

should be kept in mind to stress how important is the distinction between the impacts of this type of ridge patterns and those caused by high latitude blocking, which we are concerned about in this particular study. In fact, the balance between strong westerly zonal flows and their interruption at higher (lower) latitudes during blocking (ridge) episodes tend to dominate a large fraction of the variability of European rainfall (Hoy et al. 2014). Teleconnection indices associated with major large-scale patterns affecting the North-Atlantic and European sectors (particularly the North Atlantic Oscillation, the Eastern Atlantic and the Scandinavian pattern) are frequently used in order to explain the intra and inter-annual fluctuations of the intensity of zonal flow, and consequently of precipitation series (e.g. Trigo et al. 2008; Vicente-Serrano et al. 2009; Altava-Ortiz et al. 2010; Casanueva et al. 2014). Still, such one-dimensional monthly-based approaches hamper a deeper comprehension of more complex spatial patterns occurring at intra-monthly time scales, such as blocking systems, reinforcing the need of using more objective blocking detection schemes.

Previous studies based on these algorithms have shown that the impacts of Euro-Atlantic blocks in terms of winter precipitation regimes essentially change with latitude, with a general decrease in most of central areas of Europe, and increases at lower and higher latitudes, albeit over less extensive areas. Such changes may have significant relevance on the annual total during years with highly anomalous frequency of blocking occurrence. However, studies of European precipitation changes associated with blocking have been restricted to the winter season. In this regard, most of the European continent lacks a comprehensive and all year-round analysis on changes in precipitation due to blocking occurrence. This analysis is of particular relevance in southern areas of Europe with Mediterranean climates, where precipitation regimes during the warm season tend to be more torrential, i.e., with a higher contribution of intense and more isolated rainfall episodes to annual totals (e.g. Kutiel et al. 1996; Peñarrocha et al. 2002; Burgueño et al. 2010; Cortesi et al. 2013). Therefore, in this perspective, linking precipitation anomalies with blocking occurrence throughout the use of objective detection methods acquires particular importance. An additional asset of these methods is their versatility to address changes in surface impacts as a function of the blocking location. In this sense, previous works have shown that the distinction of separate (yet large) blocking sectors in the Euro-Atlantic sector still results in considerably different impacts at finer scales inside the Euro-Atlantic sector (Yao et al. 2014a, 2014b), and even in smaller areas such as the Iberian Peninsula (Sousa et al. 2015). Accordingly, the relevance of the specific longitudinal position of the center of a blocking system cannot be disregarded when analyzing impacts at such a large scale as for the European continent.

On the other hand, blocking impacts on European precipitation regimes have been generally characterized throughout the use of composites of either absolute or relative precipitation anomalies (e.g. Trigo et al. 2004; Masato et al. 2012). This approach focuses on changes in the mean and hence, has neglected to a large extent the importance of shifts in precipitation distributions which arise from these particular synoptic patterns. Extreme Values theory has been used to identify either changes in precipitation and temperature extremes over very confined regions (e.g., Buehler et al. 2011; Sousa et al. 2015) or shifts in temperature distributions (Sillman et al. 2011). To the best of our knowledge, the assessment of the impact of blocking patterns on the entire precipitation distribution has only been addressed outside of Europe in regions such as California (Hughes et al. 2009). The investigation of these precipitation changes can be assessed through rather simple methodologies, like the one used by Soares et al. (2014), which analyzed changes in Probability Density Functions (PDFs) of precipitation series for Portugal, in the scope of Regional Climate Models performance and future scenarios evaluation. This method follows the works of Perkins et al. (2007) and Boberg et al. (2009; 2010).

Works such as Trigo et al. (2004), Michel et al. (2012), Pfahl (2014) or Sousa et al. (2015) have also shown that the precipitation increases found in southern sectors of Europe during blocking episodes are mainly driven by dynamical features. These factors include synoptic scale processes such as increases in cyclone frequency, but there are also other thermodynamical factors which can enhance atmospheric instability at the local or mesoscale (Lolis et al. 2004; Ricard et al. 2012). Hence, smaller scale processes (e.g. latent heat fluxes) must be addressed to understand regional impacts of blocking occurrence, in line with the distinct

shaping of precipitation Probability Density Functions associated to blocking occurrence in specific sectors of the European domain.

The main objective of this work is to characterize the distinct impacts on European precipitation regimes of blocking occurrence in three different sectors, taking into account the entire distribution of precipitation series, which allows evaluating the net changes as well as the responses in precipitation intensity. The changes in the precipitation regimes of several regions will be supported by a comparison between blocked and strong zonal patterns occurring over different longitudinal sectors of the target domain. Finally, the precipitation responses will be interpreted in terms of dynamical and thermodynamical processes. The work is structured as follows: in Section 2, the datasets are presented, along with a characterization of typical atmospheric patterns during blocking episodes; in Section 3 the precipitation anomalies registered during blocked and zonal patterns are presented, followed by the main dynamical drivers associated to these atmospheric patterns in Section 4; the different responses in terms of changes in precipitation distributions due to blocked and zonal patterns are presented in Section 5; finally, a summary and discussion of the obtained results is offered in section 6.

2. Data and methods

We used daily precipitation data for Europe from the E-OBS dataset during the period 1950-2012 (Haylock et al. 2008). This European land-only daily high-resolution gridded dataset is accessible throughout the European Climate Assessment and Dataset (ECA&D), and is available on a grid with a horizontal resolution of 0.25ºx0.25º, based on the interpolation of daily observations from meteorological stations. Despite the overall good quality of this dataset we must acknowledge that this dataset has caveats in areas where the spatial distribution of stations is sparser, such as biased and over smoothed precipitation fields in some cases, as well as possible effects in extremes (e.g., Hofstra et al. 2009a,b).

The dataset from the NCEP/NCAR reanalysis (Kalnay et al. 1996), on a horizontal resolution of 2.5ºx2.5º for the 1950-2012 period is also used. The variables explicitly considered were: daily fields of 500hPa geopotential height (Z500), Lifted Index (LI) and Latent Heat Flux (LHF). In addition, several fields also from the NCEP/NCAR reanalysis were employed to compute the Integrated Water Vapor Transport between 1000hPa and 300hPa (IVT, Ramos et al. 2015) and the following catalogues of weather systems: i) blocking events (Barriopedro et al. 2006); ii) strong zonal flow days (Sousa et al. 2015); iii) extratropical cyclones for the northern hemisphere obtained by using the methodology described in Trigo (2006). These derived datasets are used to explore the blocking signatures in precipitation regimes and to interpret the role of the associated dynamical and thermodynamical processes.

The particular characteristics of the blocked and zonal days catalogues are described next. We distinguish synoptic conditions characterized by blocked patterns and strong zonal flows by objectively identifying days under such atmospheric conditions in the Eurasian sector. These methods rely on the Z500 field from the NCEP/NCAR reanalysis. The catalogue of blocked days was developed by Barriopedro et al. (2006) - further information on the methodology can be found in that work. The authors have used this and other similar blocking datasets extensively for different applications, such as to characterize blocking effects on total ozone (Barriopedro et al. 2010c) and stratospheric variability (Barriopedro and Calvo 2014), and in evaluating the impact of blocking patterns in the Iberian Peninsula using a high resolution precipitation dataset (Sousa et al. 2015).

Following the latter work, the locations of the maximum Z500 for each identified blocking pattern will hereafter be called blocking centers. The reduction of the large-scale blocked pattern to a single central gridpoint (representative of the entire blocking system) enables an objective separation of blocking in different spatial sectors. Thus, three sectors were defined: the Atlantic sector (ATL) which includes all blocking centers located in 30-0º W, the European sector (EUR), spanning 0-30º E and the Russian sector (RUS), including blocking centers positioned between 30-60ºE. Fig.1 presents the annual mean frequency

of blocking center locations in each gridpoint. We must stress that this classification of blocks into ATL, EUR an RUS types intends to assess different precipitation responses and changes in precipitation regimes purely based on the geographical location of the considered high pressure system, which strongly influences the synoptic environment associated to blocking occurrence in each considered sector. The selection of these blocking sectors is based on previous studies that have already identified distinctive features in the resulting blocking signatures (Wang et al. 2010; Masato et al. 2011; Sousa et al. 2015).

Seasonal composites of Z500 anomalies during blocking days in each sector are shown in Fig. 2. Positive Z500 anomalies centered in the respective blocking sector dominate the northern latitudes, being larger in the colder seasons for all sectors. They capture well the canonical signatures associated with blocking over its climatologically preferred sectors of occurrence in the Eurasian sector, which include eastern Atlantic, Scandinavian and the Urals, respectively. Negative anomalies of the Z500 fields are less pronounced and usually found southwards and northwards of the blocking centers, mainly during ATL blocks. Also, in this region, summer blocks display a northward extension of subtropical wave-breaking systems near the Azores high. It is important to note that some blocking events contribute to the composites of more than one sector during their lifecycle, since they tend to evolve eastwards towards Europe (Croci-Maspolli et al. 2007; Barriopedro et al. 2010a; Sousa et al. 2015).

As a complement to highlight the large impacts resulting from zonal flow reversals which occur during blocking episodes, we also computed a catalogue of days were strong zonal flow conditions occur in the same three sectors (ATL, EUR and RUS). They represent strong westerly flows and hence a large-scale atmospheric pattern that is nearly opposite to that of blocking. They were computed following very simple criteria based on several empirical thresholds imposed on the meridional mid-latitude Z500 gradients to ensure a strong westerly flow. See Trigo et al. (2004) for further details on the methodology.

Extratropical cyclones for the northern hemisphere were obtained by adapting the methodology described in Trigo (2006) and recently used to assess and intercompare the most common features of mid-latitude cyclones, including the most active regions, the most common trajectories, inter-annual variability and trends (e.g. Vicente-Serrano et al. 2011; Neu et al 2013), cyclone formation mechanisms and impacts (e.g. Liberato et al. 2012, Liberato et al. 2013). The objective cyclone identification is based on the detection of local minima in 1000 hPa geopotential height. The cyclone tracking consists on a nearest neighbour search in the previous Z1000 field, considering several thresholds: (i) within a certain area, the cyclone speed should not exceed 50 km/h in the westward direction and 160 km/h in any other. Additionally, the cyclone speed should be higher than 12 km/h. These criteria allow to include the most rapidly deepening cyclones (e.g. Xynthia, Liberato et al. 2013) and to filter the stationary cyclones; (ii) during the lifecycle the cyclone should reach a minimum central pressure corresponding to a see level pressure below 1020 hPa; (iii) a minimum lifetime of 24 hours.

3. Changes in mean precipitation rates

In order to evaluate the distinct impacts of the different blocking locations on precipitation regimes, we computed the composites for absolute and relative anomalies of daily precipitation, during blocked and zonal days, in each of the three considered sectors, at the annual and seasonal temporal scales (Figs 3 and 4). When evaluating the resulting relative anomaly composites one must bear in mind the large range of precipitation values that coexist within such a large domain as the European continent. Thus, one must take into account that similar absolute anomalies in regions with very distinct total annual precipitation climatologies have different relevance. Consequently, to ensure this distinction we first considered the

annual composites for the relative changes in precipitation during blocked and zonal days, as presented in Fig.3.

Fig.3 clearly shows that for the three considered sectors, the presence of blocking systems leads to well below average precipitation in a wide region under direct influence of the anticyclonic circulation. Maximum decreases of near 75% are recorded in northern Europe near the blocking centers, which corresponds to an almost complete cease of precipitating days. The maximum negative anomaly is well collocated with the maximum Z500 anomaly of the respective sector (Fig.2), being more extensive for EUR blocking. On the other hand, the increase in precipitation in southern areas of Europe, as well as in the Atlantic strip of Scandinavia matches well with the negative Z500 anomalies, which arise northward and southward of blocking systems (as shown in Fig.2). These positive precipitation anomalies shift eastwards with the considered blocking sector, thus following the relative west-east migration of the maximum Z500 positive anomaly (blocking center). At the annual scale, the widest positive anomalies are found for ATL blocks, during which a large portion of Iberia, Italy, and the Balkans region experience wetter than usual conditions. In particular, daily precipitation rates in southeastern Iberia almost double.
During strong zonal westerly flows these anomalies are essentially inverted, with a significant reduction in precipitation amounts at lower latitudes, particularly around the Mediterranean basin. Much less significant losses are also found for northernmost areas of Scandinavia. On the contrary, sharp increases in precipitation rates are found in most central and northern Europe, with gains close to 100% in Benelux, Germany and southern Scandinavia during strong zonal flows in the EUR sector. The difference between composites for blocked and zonal flows sharpens their opposite responses in daily precipitation anomalies, thus illustrating the very significant impacts of zonal flow reversals.
The presented changes in precipitation are in general good agreement with those in the frequency of dry days (below 1mm) - see Fig.S1 from the Supplementary Material. In Section 5, we will address in more detail how the changes in the number of wet days are distributed for different precipitation intensities.

As stated before, annual rainfall totals in the European domain range from a few hundred mm in dryer regions to several thousand mm in mountainous regions, particularly in Atlantic coastal areas (Haylock et al. 2008). This must be taken into account when analyzing relative anomalies, as a change of 50% per day in a dry region/season corresponds to a much lower absolute precipitation anomaly than in a corresponding wet region. Therefore, we now present (Fig. 4) the corresponding seasonal analysis of Fig.3 but based on the precipitation absolute anomalies at the seasonal scale. In this case, we summarize the results presenting the difference in daily rates between blocking and strong zonal flow days.

When using absolute anomalies, the relative changes are emphasized in regions where seasonal precipitation amounts are high, as for example in central and northern Europe during most of the year, or in easternmost interior areas during the warm seasons. Nevertheless, increases of 2-3mm per day are significant in relatively dry areas (such as southernmost Europe), as previously depicted in Fig.3. When blocked conditions prevail, precipitation losses in the UK and Central Europe are quite striking throughout the year. Summer precipitation responses often embrace lower spatial extensions; however, in some regions such as the northernmost countries and Russia - where precipitation in form of snow is often recorded in colder months - the summer deficits represent the largest changes.

This seasonal analysis also helps distinguish seasonal precipitation responses that are masked at the annual scale. For example, during summer, blocking systems and their associated impacts shift north, and rainfall increases in parts of continental Europe - suggesting a rise in convective precipitation during summer blocks, , as it will be discussed further ahead.

4. Synoptic and dynamics associated to different blocking locations

To better understand the processes triggering the precipitation anomalies associated with blocking (particularly relevant in southern Europe) we analyzed the changes in the frequency of extratropical cyclonic activity occurring during blocked and zonal regimes. According to Neu et al. (2013) a cyclone refers to a point (the cyclone center) identified on the Earth's surface at a certain time using a certain methodology. The annual mean climatological frequency of extratropical cyclone center locations in the Euro-Atlantic-Russian sectors is shown in the top panel of Fig.5, along with their relative anomalies (in %) during blocked and zonal events in each sector.

A clear increase in cyclonic activity (non-stationary near-surface systems) in southwestern Europe is found during ATL blocks (Fig.5, middle left), contrasting with an almost complete cutback in the UK area, where cyclonic activity is almost non-existent during blocking patterns (relative changes near 100%). This decrease shifts eastwards as we consider blocking sectors further east. In the particular cases of EUR and RUS blocks, increases in cyclone frequency are also found south of the blocking structures, although more spatially confined and much less pronounced. These changes are in agreement with the well-known blocking effect on storm-tracks and the resulting split in two branches - north and south of the blocking high. During zonal patterns consistent increases in cyclone activity are found at higher latitudes, ranging from Iceland to eastern areas of Scandinavia and northern Russia, along with an eastward extension of the strongest branch of the Jetstream. On the southern flank of the Jetstream mean location we find negative anomalies in the frequency of cyclones. These occur over large portions of Western and Central Europe during strong westerly flows in the ATL and EUR, which in the specific case of the former synoptic pattern contrast with simultaneous increases (reaching 50%) in eastern Mediterranean areas. Modest increases in extratropical cyclone paths at lower latitudes are also found during strong westerly flow regimes. Nevertheless, these changes tend to be comparatively smaller than those during blocking. Similar spatial patterns have been found for the changes in cut-off lows frequency during blocked/zonal conditions (Sousa et al. 2015; Nieto et al. 2007).

As expected, the southward shift in cyclonic activity during blocking episodes is in fair agreement with the decrease (increase) in precipitation in northern (southern) Europe. This impact is particularly striking during ATL blocks, which exert the largest influence on the track of storm approaching Europe, and accordingly, on the European moisture sources of the Atlantic Ocean, as it will be detailed further ahead. On the other hand, the modest increases in cyclone frequency over some Mediterranean areas during zonal flows are not accompanied by significant rises in precipitation rates (Fig. 3).

To complement the obtained changes in cyclonic activity and deep further in the processes behind the precipitation responses, we computed composites of Z500, LI, and IVT (and the corresponding mean horizontal transport of IVT) for blocked and zonal days. The anomalous fields of these variables are shown simultaneously in Fig.6, in order to evaluate concurrently the dynamic and thermodynamical processes (including moisture fluxes and atmospheric instability).

The composites during strong zonal flow days (Fig.6, middle row) reveal a stretching of the high moisture content corridor from the Atlantic towards each considered sector, although in the case of the RUS sector, moisture income towards this area is relatively modest. These extensions towards each sector are on the overall quite coherent with the cyclonic signatures and the precipitation anomalies during zonal days previously shown (Fig.3). On the other hand, blocking structures obstruct these moisture fluxes (Fig.6, upper row), being most of the moisture transport deflected northwards. In the case of ATL blocks, these fluxes are diverted far from continental Europe and the UK, while during EUR blocks the northward deflection of the moisture corridor occurs over Ireland towards Scandinavia. Moisture transport anomalies during RUS blocks are less striking, which agrees with the fact that larger precipitation anomalies in this sector are confined to summer (Fig.4), when moisture fluxes are reduced. For the three blocking sectors, there is also a modest transport towards lower latitudes (Mediterranean areas) through the southern flank

of the blocking systems. In agreement with the precipitation differences between blocked and zonal patterns, the corresponding difference in moisture fluxes at the annual scale (Fig.6, lower row) clearly shows that a shift from a westerly flow to blocked pattern results in an overall substantial decrease in moisture availability over western and central areas of Europe, and in a significant increase in northernmost Scandinavian areas.

The precipitation increases in southern Europe during blocking episodes do not reflect significant anomalies in available moisture. Instead, for southernmost latitudes, atmospheric instability (depicted by the Lifted Index) appears to relate better with precipitation anomalies, as evidenced in the blocking minus zonal flow composites (bottom panels of Fig.6). Moreover, these changes in LI are spatially consistent with the changes in cyclonic activity frequency, suggesting potential effects in the frequency of extreme precipitation days (as it will be analyzed in Section 5) in the regions located at the southern flank of blocking structures (i.e. in Mediterranean areas). Thus, moisture availability is not a major constrain to the occurrence of significant precipitation events in Southern Europe, at least at the annual scale. On the other hand, the small increases in cyclonic activity in the Mediterranean area which are found during zonal days (Fig. 5) are not collocated with the positive LI changes (located further north), therefore supporting the weak precipitation effectiveness of low-latitude weather systems under zonal flows. All these facts reinforce the major role played by atmospheric instability on the precipitation regimes of southern Europe, and its gradual loss of importance as we move north, where stratiform precipitation and moisture availability tend to dominate.

Despite cyclonic activity increases in northern Europe extend to parts of Central Europe during ATL blocks (Fig. 5), the simultaneous reduction in moisture fluxes at these latitudes explains the decrease in precipitation that can be found in areas such as southern France, parts of central Europe, or even northwestern sectors of the Iberian Peninsula. In this sense, it is important to stress that frontal precipitation associated to extratropical cyclones tends to occur to the south of the cyclone center. As an example concerning the latter region, Sousa et al. (2015) noted that a large fraction of the precipitation that occurs in this area depends on frontal systems linked to cyclone centers located at higher latitudes, and whose frequency is strongly reduced during blocking situations. The same rationale can be applied to other regions as France and central parts of Europe during blocking events in the EUR sector. Thus, while at higher latitudes, the blocking-related decreases in precipitation are in good agreement with an obstruction of storm-tracks and associated moisture corridors, in southern areas, the agreement between blocking-related rainfall increases (Fig.4) and above average atmospheric instability suggests a shift towards more extreme precipitation regimes.

Overall, the seasonal composites (Fig.7) resemble the annual, although a generalized northward shift can be noted during the warm season - in good agreement with the corresponding migration of the seasonal precipitation anomalies (Fig.4). The pattern of enhanced atmospheric instability in the areas southwards of blocking systems is considerably larger in warmer months. During spring and summer the increase in instability is quite striking west of Iberia (during ATL blocks), as well as in southern France and western Mediterranean areas (during EUR blocks). Interestingly, during summer, an outstanding rise in atmospheric instability during RUS blocks covers a wide domain spanning from Turkey to Scandinavia. The fact that this pattern is essentially restricted to summer explains its absence at the previous annual scale analysis. In effect, during summer some continental areas display precipitation decreases under blocked conditions, despite significant increases in atmospheric instability. We hypothesize that the summer enhancement in atmospheric instability during blocked days must be insufficient to overwhelm the moisture inflow reduction associated with this atmospheric pattern. Thus, once again we find that the precipitation responses in northern areas of Europe are well explained by changes in moisture availability. Nevertheless, some mid-latitude continental areas show a seasonal shift towards wetter conditions during summer and autumn blocks, despite the overall reduction in moisture inflow. These regional warm season changes are concurrent with remarkable increases in LI and hence, the reasoning could be quite comparable to the one presented for southern Europe (essentially driven by atmospheric instability. In summary, this balance between contrasting responses in terms of moisture flows and atmospheric instability between northern and

southern Europe is, overall, well explained by a dominant role of moisture fluxes in the former, and of atmospheric instability in the latter, whose influence extends further north into continental Europe during the warmer months.

The atmosphere-ocean coupling must be also considered in this context. In fact, variables such as Sea Surface Temperature anomalies and Latent Heat Fluxes (hereafter LHF) may play a role on thermodynamic processes at both local scale (such as small scale convective systems), and synoptic scale, such as cyclone life-cycles (Grams et al. 2011). As previously shown, LI changes are not always associated to concurrent changes in atmospheric circulation (e.g. cyclones), and hence, the underlying processes behind these LI changes (particularly important in southern areas) should be explored. Thus, we have analyzed changes in LHF during blocked and zonal patterns, as presented in Fig.8.

As it can be observed in the top panel of Fig.8, the highest mean values of LHF (at the annual scale) are observed over the equatorial areas and the Gulf Stream in the Western Atlantic. These areas with high rates of oceanic evaporation are the main large-scale sources of moisture content originated in the Atlantic which are carried towards Europe by typical westerly flows (Gimeno et al. 2013). Other regions, such as the Mediterranean area, may also be important sources of moisture for regional precipitation throughout evaporative processes (Gimeno, 2010; 2012). Subsequently, we analyzed LHF anomalies during blocked or zonal synoptic patterns, as changes in evaporative rates should not be disconnected from the thermodynamic processes related with precipitation (particularly convection).

As shown in Fig.8, strong zonal flows are related to above average LHF at higher latitudes, particularly notable in the vicinity of the UK during ATL events, but also in the North Sea and Baltic Sea during EUR and RUS zonal flow episodes, respectively. On the contrary, at lower latitudes, these zonal regimes result in below average LHF. During blocked conditions, there is an overall opposite response in terms of LHF anomalies. For example, during ATL blocks, a large area surrounding Iberia shows higher values of LHF (with maximum expression in the Gulf of Biscay). During EUR blocks this pattern shifts eastwards towards the eastern Mediterranean (particularly in the Aegian Sea), while during RUS blocks positive anomalies are restricted to the Black Sea.

This pattern of above average LHF in the southern flank of blocking systems may reflect enhanced evaporative processes under the advection of cooler air from higher latitudes due to the easterly/northeasterly synoptic flow. On the other hand, strong westerly flows extending to the surface level may explain the increased LHF at higher latitudes during zonal regimes. Note that the regions of increased LHF during blocked conditions do not display concurrent changes in atmospheric circulation, but they agree with the regions experiencing increased precipitation. In this context, positive LHF anomalies could help explain thermodynamic processes which regionally enhance atmospheric instability in southern areas of Europe during blocking episodes. Taking the Iberian Peninsula as an example, in Fig.S2 of the Supplementary Material we present the forward trajectories of air parcels (at different altitudes) originated in areas where the maximum LHF anomaly was found (e.g., the Gulf of Biscay) for a subset of days under ATL blocking. This pattern favors the transport and elevation of air parcels (originally at lower levels in the region with above normal evaporation) towards Iberia, thus possibly establishing a positive feedback process between evaporative and convective processes, and contributing, at least partially, to the observed rainfall increases in the region.

5. Shifts in precipitation distributions

In the previous sections we analyzed net precipitation changes in Europe associated to distinct atmospheric circulation patterns. Still, it is important to understand the underlying shifts in different precipitation regimes (or intensities), which can be addressed looking at precipitation distributions, or commonly

designated PDF changes. In this section we perform a comprehensive assessment of modifications in precipitation distributions in some representative areas (identified in the boxes in Fig.1) following a similar scheme as the one presented in Soares et al. (2014), and consisting in the next steps:

i) For each box presented in Fig.1, we pooled together all the gridpoints, and then computed frequency histograms for wet days (days with rainfall above 1mm) for 1mm bins, without distinguishing weather regimes ($HIST_{ALL}$);
ii) The frequency of each of these bins has been multiplied by its precipitation value, in order to obtain its relative contribution to the total precipitation climatology ($CONT_{ALL}$) of each box;
iii) The previous procedure was also applied to wet days under each specific weather regime and for each sector (thus obtaining $CONT_{BLOCK}$ and $CONT_{ZONAL}$);
iv) The difference between the bin contributions under each weather regime and the corresponding all-days bin was then computed, in order to obtain the relative change in the contribution of different daily precipitation intensities to the total precipitation anomaly ascribed to the specific weather regime, according to:

$$(CHANGE_{Block}) = \frac{CONT_{BLOCK} - CONT_{ALL}}{NDAYS_{BLOCK}} \quad (1)$$

$$(CHANGE_{Zonal}) = \frac{CONT_{ZONAL} - CONT_{ALL}}{NDAYS_{ZONAL}} \quad (2)$$

The computation described in equations (1) and (2) has been performed for all three sectors considered previously (ATL, EUR and RUS), and *NDAYS* represents the number of wet days occurring in each of these specific weather regimes.

Since the sample sizes for each specific weather regime and for each sector are different (and much smaller than the all-days sample size) we have applied a bootstrapping technique to enable a fair comparison between them. For each weather regime, the method estimates $HIST_{ALL}$ for subsamples of days with the same size as that of the specific weather regime. Thus, for a given weather regime having *NDAYS* as sample size, we randomly selected *NDAYS* from the complete series and obtained the corresponding histogram, to perform an unbiased comparison. This random process was repeated 1000 times, and the average of the resulting histograms was taken as the final $HIST_{ALL}$.

The precipitation distributions of the four selected European regions and their shifts associated with the occurrence of blocking and strong westerly flows over each sector are shown in Figs.9-12. In these figures, the upper panel shows the histogram of daily precipitation for all wet days (above 1mm, $HIST_{ALL}$) and the black curves show the contribution of each bin to the total precipitation ($CONT_{ALL}$), thus highlighting the daily intensities that are more relevant to the total rainfall of each specific region. The middle panels show the relative changes for each bin under each specific weather regime ($CHANGE_{Block}$ and $CHANGE_{Zonal}$, distinguishing between the three sectors considered), in order to compare the impacts that each atmospheric pattern promotes in different precipitation intensities. Finally, the lower panels show the cumulative relative changes from the previous panels, with the impacts of each considered weather pattern on the total precipitation distribution of the considered location. Please note the different y-axis scales in Fig.9-12.

This approach enables a deeper assessment of the contrasting anomalies found in the precipitation composites (Fig.3 and 4) for areas such as the UK (Fig.9) or the Iberian Peninsula (Fig.10). As stated before, ATL and EUR blocked patterns reduce daily precipitation rates in the UK and foster them on most of the Iberian Peninsula, while the opposite result is found for strong zonal flow days. The analysis of Fig.9 provides a more detailed view of these differences, as it clarifies that blocked patterns in the ATL sector drastically reduce the number of moderate rainfall days in the UK region (below the 90th percentile), and

increase the frequency of low precipitation days, as compared to the climatology. The latter have a relatively minor contribution for the precipitation totals, while the former impinge a very large impact on the accumulated relative changes of the precipitation distribution (Fig.9, lower panel), with the total effect being a reduction of 40% in annual precipitation. On the contrary, strong zonal patterns (particularly in the ATL and EUR sectors) induce an increase of the highly-contributing precipitation bins (those near the median of the distribution), resulting in positive cumulative changes, in clear agreement with the composites of the previous section. Thus, ATL patterns are the most efficient in triggering shifts in precipitation distributions in the UK.

On the other hand, the differences in Iberian precipitation (Fig.3) during blocked (zonal) days in the ATL and EUR sectors are associated to an increase (decrease) in days with precipitation amounts above the 50^{th} percentile (Fig. 10). Contrarily to the UK, where blocked and zonal flows have minor impacts in the occurrence of extreme precipitating events, in the Iberian Peninsula ATL and mainly EUR blocks are associated with a substantial shift in extreme events (Fig.10, middle panel), which largely influences the annual total differences in precipitation (Fig.10, lower panel). This is a strong evidence of the impact that blocked patterns have on the occurrence of intense to extreme precipitation days in this area, which are essentially driven by atmospheric instability, as referred in Section 4. These results help distinguish the utterly different precipitation regimes, and the underlying processes, that dominate annual rainfall totals at different European latitudes. Still, we must bear in mind the existence of large gradients in precipitation regimes that characterize some areas (particularly in southern Europe). Such different responses across regions and seasons, result in a smoothed signal in the annual balance for the entire region. In the particular case of the Iberian Peninsula, different local responses from the overall region's signals are found in northwestern areas during the wet season (Sousa et al. 2015), as shown in Fig.S3 and S4 of the Supplementary Material.

The contrasting results between the UK and Iberian Peninsula shifts in the precipitation distributions are similar to those found between central/northern Europe against the central Mediterranean areas, the main difference residing on the zonal (blocking) sector with most important differences, which in the latter cases correspond to the EUR sector. Thus, zonal (blocked) conditions relate to an overall increase (decrease) in the number of moderate rainfall days (largest differences around 5 mm/day rates) in most of central/northern Europe, while the opposite response is found at lower latitudes, where differences are more associated to the higher percentiles of daily precipitation intensity. Taking into account the similarity with the previous cases, we opted to remit the corresponding figures (S5 and S6) to the Supplementary Material.

We also explored the shifts in the seasonal distributions. Overall, the results indicate a latitudinal dependent behavior. Northern regions of Europe exhibit qualitatively coherent responses to weather systems through the year, although the cumulative changes can display seasonal variations, following the seasonal cycle of precipitation and the factors that cause precipitation anomalies therein (cyclonic activity and moisture availability). As an example, we decided to present the differences in the summer precipitation distribution of the Russian box to emphasize the huge impact that summer blocking episodes exert on the climate of this region (Fig.11). As in other northern/central European areas, the positive (negative) cumulative changes that arise from zonal (blocked) flows over this region are strongly influenced by variations in the number of moderate rainfall days.

On the other hand, the shifts in the precipitation distribution of southern European areas are more likely to be seasonal dependent, as the seasonal cycle in precipitation is larger and the relative contribution of extreme precipitation to the annual total is more important than in northern Europe. Fig.12 shows the PDF changes at the annual scale for Turkey. Significant differences occur in a wide range of percentiles, including the highest ones (above the 95^{th}). However, there are clearly contrasting responses between winter and summer weather patterns (see Figs. S7 and S8 from the Supplementary material. There is not a clear opposite response to zonal or blocked flows, nor a coherent signal through the year. This fact suggests an important heterogeneity in precipitation regimes at both intra-annual and spatial scales in the region, when

compared to other European areas, and in particular with other Mediterranean sectors (Sousa et al. 2011). The fact that some other European areas do not show significant differences in the annual mean precipitation responses to blocked/zonal may be due to the co-existence of similar contrasting signals, either in different seasons, or at different precipitation intensities of the distribution.

In summary, the presented cases denote that precipitation regimes in southern Europea are more dependent (than those at higher latitudes) of shifts in the higher percentiles of the daily rainfall intensity. In addition, heterogeneities at both spatial and temporal scales are also much more important than in northern Europe, where distributions tend to be qualitatively similar throughout the year. Consequently, in northern regions, annual analyses of the precipitation distribution shifts are generally sufficient to examine the distinct impacts of blocked and zonal episodes, as the shifts in highly-contributing moderate rainfall days prevail in these regions throughout the year.

6. Discussion and Conclusions

We have performed a pan-European analysis on the impacts of blocking episodes and strong zonal flows on European precipitation regimes and the physical mechanisms associated. Unlike previous studies, we have described the impact in annual and seasonal precipitation, thus including seasons other than winter, which has been the focus of previous assessments. We first analyzed composites for precipitation anomalies, and afterwards, the precipitation distribution shifts over major regional domains, considering in all cases the effects of large scale circulation anomalies over three different areas of occurrence (mid-Atlantic, Europe and Russia).

Overall, the results indicate significant opposite precipitation responses to blocking occurrence between northern and southern regions of the continent. Positive net changes are found in southernmost areas, while negative net changes occur in most central and northern regions of Europe – exception made for the Atlantic strip of Scandinavia where variations in precipitation present the same signal response as in southern Europe. The location of the largest precipitation anomalies follows well the positioning of the blocking centers, migrating eastward as we move from the Atlantic to the Russian sector. On the other hand, during strong westerly flows, the anomalies of this north-south dipole are reversed, resulting in precipitation gains (decreases) at higher (lower) latitudes. In the areas under direct blocking influence, the substantial decrease in precipitation rates (reaching in some cases around 75%) extends throughout the year, including areas where annual rainfall totals depend more on warm season's precipitation. In particular, the dramatic decrease in Russian precipitation during spring and summer blocking episodes gains particular relevance under the scope of recent noticeable events, such as the mega-heatwave of 2010 (Barriopedro et al. 2011). Our results reinforce the potentially outstanding impact of prolonged blocking episodes occurring over continental areas in terms of water availability (e.g., the role of Russian blocks on the complex feedback processes between pre-conditioning soil moisture deficits and summer heatwaves enhancement, Miralles et al. 2014; García-Herrera et al. 2010).

The presence of blocking systems results in a bifurcation of storm-tracks north and south of their usual paths, as already described by Trigo et al. (2004) or Walter and Graf (2005). In large parts of central and northern Europe, where frontal systems associated to synoptic-scale disturbances usually prevail, these storm-track shifts are responsible for the previously referred rainfall deficit due to the subsequent significant decreases in cyclone frequencies and moisture transport. Contrariwise, during days characterized by strong zonal flow, our results demonstrate an increase in cyclonic activity and moisture transport towards northern and central Europe, concurring with a rise in rainfall totals, associated to a stronger than usual Jetstream. In agreement with this main driver of precipitation anomalies in northern and central Europe, the strongest effects are observed under the occurrence of circulation anomalies centered in the Atlantic and European sectors, which exert a major influence on the storm-tracks and moisture advection inland.

On the other hand, in southern Europe, the branch of storm-tracks deflected southwards due to blocking occurrence is responsible for above average cyclonic activity. Again, this effect is particularly relevant for blocking centers located in the Atlantic sector, resulting in twice as much cyclonic activity in the Iberian Peninsula area. Although not so striking, increases in cyclone frequency extend throughout many Mediterranean areas for other blocking locations. Quite the opposite, rainfall deficits in southern Europe are found for strong westerly flows, particularly in western and central Mediterranean areas.

While the rainfall increases over southern Europe during blocking agree with cyclonic activity anomalies, we have shown that they are better explained by increases in atmospheric instability, which are particularly notable in the southern flank of blocking systems. This process is not particularly dependent of high moisture contents, as our analysis shows that these blocking-related rainfall increases are concurrent with below average moisture influxes towards Europe. This emphasizes the more convective nature of precipitation regimes of southern European countries, when compared to a much more relevant contribution of frontal/stratiform systems at higher latitudes. These results lead us to perform a more regionalized assessment of precipitation changes and to highlight the meridional variation in precipitation responses and associated mechanisms. In this regard, we went further than previous studies by analyzing changes in the seasonal and annual precipitation distributions for a number of boxes in northern and southern Europe, during blocked and zonal regimes.

We show that the overall negative net changes in precipitation in most sectors of central/northern Europe are essentially driven by the substantial drop in the mid-percentiles of the distribution (i.e., moderate rainfall days), which strongly contribute to the cumulative totals. Inversely, during days characterized by intense zonal flow, an increase in the mid-percentiles of daily precipitation rates highlights the vital role of synoptic-scale frontal systems and their association to a stronger Jetstream and the Atlantic moisture inflow. In contrast, in southern European areas, the increases in precipitation rates during blocking episodes are mostly related with increases in the mid to high percentiles of the precipitation distribution, in some cases particularly striking above the 90^{th} and 95^{th} percentiles. This clearly shows an increase in the probability of heavy to extreme precipitation days during blocked patterns, confirming the role of convective processes in the blocking-related precipitation anomalies of southern Europe. Given the significant contribution of heavy precipitation days to annual totals in this region, our results highlight an outstanding role of blocked patterns on the inter-annual variability of southern European rainfall regimes.

In most areas, the synoptic patterns and precipitation responses are quite coherent throughout the year However, the involved mechanisms differ in magnitude and spatial extent from season to season and affected areas. In particular, blocking occurrence and the associated increase in atmospheric instability (and consequently in convective processes) to the south/southeast of blocking centers shift northward during summer, and as a consequence, positive precipitation anomalies also extend further north than during other seasons. Besides, we have also verified that while precipitation responses during blocked/zonal regimes are spatially coherent in central and northern Europe, the responses in southern regions are more complex. In this area, opposite responses within relatively small domains (and/or between different seasons) can be masked on the annual analysis (e.g. Iberia and Turkey).

Finally, we discussed how processes such as latent-heat-fluxes may be determinant to both cyclogenesis and local feedback processes. In fact, blocked atmospheric patterns are associated with above average evaporation in specific sectors, which may enhance atmospheric instability and/or provide a local moisture source for precipitation. In this context, parcel tracing and other ocean-atmosphere processes should be analyzed in more depth for a deeper assessment of local-scale processes, which may be particularly relevant in southern European areas.

Acknowledgments

Pedro M. Sousa was supported by the Portuguese Science Foundation (FCT) through a doctoral grant (SFRH/BD/84395/2012).

Alexandre M. Ramos was also supported by FCT in a postdoctoral grant (FCT/DFRH/SFRH/BPD/84328/2012).

Pedro M.M. Soares thanks the Portuguese Science Foundation (FCT) for funding under Project SOLAR - PTDC/GEOMET/7078/2014

This work was partially supported by FEDER funds through the COMPETE (Programa Operacional Factores de Competitividade) Programme and by national funds through FCT (Fundação para a Ciência e a Tecnologia, Portugal) through project STORMEx FCOMP-01-0124-FEDER-019524 (PTDC/AAC-CLI/121339/2010).

We acknowledge the E-OBS dataset from the EU-FP6 project ENSEMBLES (http://ensembles-eu.metoffice.com) and the data providers in the ECA&D project (http://www.ecad.eu).

The authors gratefully acknowledge the NOAA Air Resources Laboratory (ARL) for the provision of the HYSPLIT transport and dispersion model and/or READY website (http://www.ready.noaa.gov) used in this publication.

7. References

Altava/Ortiz V, Llasat M, Ferrari E, Atencia A, Sirangelo B (2010) Monthly rainfall changes in Central and Western Mediterranean basins, at the end of the 20th and beginning of the 21st centuries. International Journal of Climatology 31 (13): 1943-1958. doi: 10.1002/joc.2204

Anstey JA, Davini P, Gray LJ, Woollings TJ, Butchar N, Cagnazzo C, Christiansen B, Hardiman SC, Osprey SM, Yang S (2013) Multi-model analysis of Northern Hemisphere winter blocking: Model biases and the role of resolution. Journal of Geophysical Research: Atmospheres 118: 3956–3971. doi:10.1002/jgrd.50231

Barnes EA, Slingo J, Woollings T (2012) A methodology for the comparison of blocking climatologies across indices, models and climate scenarios. Climate Dynamics, 38: 2467-2481, doi:10.1007/s00382-011-1243-6

Barriopedro D and Calvo N (2014). On the Relationship between ENSO, Stratospheric Sudden Warmings, and Blocking. Journal of Climate 27 (12): 4704-4720. doi: 10.1175/JCLI-D-13-00770.1

Barriopedro D, García-Herrera R, Lupo AR, Hernández E (2006) A climatology of Northern Hemisphere blocking. J Clim 19: 1042–1063. doi: 10.1175/JCLI3678.1

Barriopedro D, García-Herrera R, Trigo RM (2010a) Application of blocking diagnosis methods to General Circulation Models. Part I: A novel detection scheme. Climate Dynamics 35: 1373-1391. doi: 10.1007/s00382-010-0767-5

Barriopedro D, García-Herrera R, González-Rouco JF, Trigo RM (2010b) Application of blocking diagnosis methods to General Circulation Models. Part II: model simulations. Climate Dynamics, 35 (7-8), 1393-1409. doi: 10.1007/s00382-010-0766-6

Barriopedro D, Antón M, García JA (2010c) Atmospheric blocking signatures in total ozone and ozone mini-holes. Journal of Climate 23 (14): 3967-3983. doi: 10.1175/2010JCLI3508.1.

Barriopedro D, Fischer EM, Luterbacher J, Trigo RM, García-Herrera R (2011) The hot summer of 2010: redrawing the temperature record map of Europe. Science 332: 220–224. doi: 10.1126/science.1201224

636 Boberg F, Berg P, Thejll P, Gutowski WJ, Christensen JH (2009) Improved confidence in climate change
637 projections of precipitation evaluated using daily statistics from the PRUDENCE ensemble. Climate
638 Dynamics 32(7–8): 1097–1106. doi:10.1007/s00382-008-0446-y

639 Boberg F, Berg P, Thejll P, Gutowski WJ, Christensen JH (2010) Improved confidence in climate change
640 projections of precipitation further evaluated using daily statistics from ENSEMBLES models. Climate
641 Dynamics 35: 1509–1520. doi: 10.1007/s00382-009-0683-8

642 Buehler T, Raible CC, Stocker TF (2011) The relationship of winter season North Atlantic blocking
643 frequencies to extreme cold or dry spells in the ERA-40. Tellus Ser. A 63: 212–222. doi:10.1111/j.1600-
644 0870.2010.00492.x

645 Burgueno A, Martinez MD, Serra C, Lana, X (2010) Statistical distributions of daily rainfall regime in
646 Europe for the period 1951-2000. Theoretical and Applied Climatology 102: 213-226. doi:
647 10.1007/s00704-010-0251-5

648 Casanueva A, Rodríguez-Puebla C, Frías MD, González-Reviriego N (2014) Variability of extreme
649 precipitation over Europe and its relationships with teleconnection patterns. Hidrology and Earth System
650 Sciences 18 (2): 709-725. doi: 10.5194/hess-18-709-2014

651 Cortesi N, Trigo RM, Gonzalez-Hidalgo JC, Ramos AM (2013) Modelling monthly precipitation with
652 circulation weather types for a dense network of stations over Iberia. Hidrology and Earth System Sciences
653 17 (2): 665-678. doi: 10.5194/hess-17-665-2013

654 Croci-Maspoli M, Schwierz C, Davies HC (2007) Atmospheric blocking: space-time links to the NAO and
655 PNA. Clim Dyn 29: 713–725. doi: 10.1007/s00382-007-0259-4

656 Davini P, Cagnazzo C, Neale R, Tribbia J (2012) Coupling between Greenland blocking and the North
657 Atlantic Oscillation pattern. Geophys. Res. Lett. 39: L14701. doi:10.1029/2012GL052315.

658 Didier Ricard, V. Ducrocq, Ludovic Auger (2012). A Climatology of the Mesoscale Environment
659 Associated with Heavily Precipitating Events over a Northwestern Mediterranean Area. Journal of Applied
660 Meteorology and Climatology (Impact Factor: 2.02). 03/2012; 51(3):468-488. DOI: 10.1175/JAMC-D-11-
661 017.1

662 Draxler RR and Rolph GD (2003) HYSPLIT (HYbrid Single-Particle Lagrangian Integrated Trajectory)
663 Model access via NOAA ARL READY Website (http://www.arl.noaa.gov/HYSPLIT.php). NOAA Air
664 Resources Laboratory, Silver Spring, MD.

665 Dunn-Sigouin E and Son S (2013) Evaluation of Northern Hemisphere Blocking Climatology in the Global
666 Environment Multiscale Model. Monthly Weather Review 141 (2): 707-727. doi: 10.1175/MWR-D-12-
667 00134.1

668 Garcia-Herrera R, Diaz J, Trigo RM, Luterbacher J, Fischer EM (2010). A Review of the European Summer
669 Heat Wave of 2003. Critical Reviews in Environmental Science and technology 40: 267-306. doi:
670 10.1080/10643380802238137

671 Grams CM, Wernli H, Bottcher M, Campa J, Corsmeier U, Jones SC, Keller JH, Lenz CJ, Wiegand L
672 (2011) The key role of diabatic processes in modifying the upper-tropospheric wave guide: a North Atlantic
673 case-study. Quarterly Journal of the Royal Meteorological Society 137 (661): 2174-2193 (B). doi:
674 10.1002/qj.891

675 Gimeno L, Nieto R, Trigo RM, Vicente S, Lopez-Moreno JI (2010) Where does the Iberian Peninsula
676 moisture come from? An answer based on a Largrangian approach. Journal of Hydrometeorolog, doi:
677 10.1175/2009JHM1182.1 (Published)

Gimeno L, Stohl A, Trigo RM, Domínguez F, Yoshimura K, Yu L, Drumond A, Durán-Quesada AM, Nieto R (2012) Oceanic and Terrestrial Sources of Continental Precipitation. Reviews of Geophysics 50: RG4003. doi:10.1029/2012RG000389

Gimeno L, Nieto R, Drumond A, Castillo R, Trigo RM (2013) Influence of the intensification of the major oceanic moisture sources on continental precipitation. Geophysical Research Letters 40: 1443-1450. doi:10.1002/grl.50338

Haylock MR, Hofstra N, Klein Tank AMJ, Klok EJ, Jones PD, New M (2008) A European daily high-resolution gridded dataset of surface temperature and precipitation. Journal of. Geophysical Research (Atmospheres) 113: D20119. doi:10.1029/2008JD10201

Hofstra N, Haylock M, New M, Jones PD (2009), Testing E-OBS European high-resolution gridded data set of daily precipitation and surface temperature. Journal of Geophysical Research 114: D21101. doi: 10.1029/2009JD011799

Hofstra N, New M, McSweeney C (2010) The influence of interpolation and station network density on the distributions and trends of climate variables in gridded daily data. Climate Dynamics 35 (5): 841-858. doi: 10.1007/s00382-009-0698-1

Hoy A, Schucknecht A, Sepp M, Matschullat J (2014) Large-scale synoptic types and their impact on European precipitation. Theoretical and Applied Climatology 116 (1): 19-35. doi: 10.1007/s00704-013-0897-x

Hughes M, Hall A, Fovell RG (2009) Blocking in Areas of Complex Topography, and Its Influence on Rainfall Distribution. Journal of the Atmospheric Sciences 66 (2): 508-518. doi: 10.1175/2008JAS2689.1

Kalnay E, Kanamitsu M, Kistler R, Collins W, Deaven D, Gandin L, Iredell M, Saha S, White G, Woollen J, Zhu Y, Chelliah M, Ebisuzaki W, Higgins W, Janowiak J, Mo KC, Ropelewski C, Wang J, Leetmaa A, Reynolds R, Jenne R, Joseph D (1996) The NCEP/NCAR 40-Year Reanalysis Project. Bulletin of the American Meteorological Society 77 (3): 437–471. doi: 10.1175/1520-0477(1996)077<0437:TNYRP>2.0.CO;2

Kutiel H, Maheras P, Guika S (1996) Circulation and extreme rainfall conditions in the eastern Mediterranean during the last century. International Journal of Climatology 16: 73–92. doi: 10.1002/(SICI)1097-0088(199601)16:1<73::AID-JOC997>3.0.CO;2-G

Liberato MLR, Ramos AM, Trigo RM, Trigo IF, Durán-Quesada AM, Nieto R, Gimeno L (2012) Moisture Sources and Large-Scale Dynamics Associated With a Flash Flood Event, in Lagrangian Modeling of the Atmosphere (eds J. Lin, D. Brunner, C. Gerbig, A. Stohl, A. Luhar and P. Webley). Geophys. Monogr. Ser. 200: 111-126, American Geophysical Union, Washington, DC. doi: 10.1029/2012GM001244

Liberato MLR, Pinto JG, Trigo RM, Ludwig P, Ordóñez P, Yuen D, Trigo IF (2013) Explosive development of winter storm Xynthia over the Subtropical North Atlantic Ocean. Natural Hazards and Earth System Sciences 13: 2239-2251. doi:10.5194/nhess-13-2239-2013

Lolis CJ, Bartzokas A, Katsoulis BD (2002) Relation between sensible and latent heat fluxes in the Mediterranean and precipitation in the Greek area during winter. International Journal of Climatology 24 (14): 1803-1816. doi: 10.1002/joc.1112

Masato G, Hoskins BJ, Woollings TJ (2012) Wave-breaking characteristics of midlatitude blocking. Quarterly Journal of the Royal Meteorological Society 138 (666): 1285-1296 (A). doi: 10.1002/qj.990

Masato G, Hoskins BJ, Woollings T (2013) Winter and Summer Northern Hemisphere Blocking in CMIP5 Models. Journal of Climate 26 (18): 7044-7059. doi: 10.1175/JCLI-D-12-00466.1

Matsueda M, Mizuta R, Kusunoki S (2009) Future change in wintertime atmospheric blocking simulated using a 20-km-mesh atmospheric global circulation model. J. Geophys. Res., 114: D12114, doi: 10.1029/2009JD011919

Michel C, Riviere G, Terray L, Joly B (2012) The dynamical link between surface cyclones, upper-tropospheric Rossby wave breaking and the life cycle of the Scandinavian blocking. Geophysical Research Letters (39): L10806. doi: 10.1029/2012GL051682

Miralles DG, Teuling AJ, van Heerwaarden CC, de Arellano JVG (2014) Mega-heatwave temperatures due to combined soil desiccation and atmospheric heat accumulation. Nature Geoscience 7 (5): 345-349. doi: 10.1038/NGEO2141

Neu U, Akperov MG, Bellenbaum N, Benestad R, Blender R, Caballero R, Cocozza A, Dacre HF, Feng Y, Fraedrich K, Grieger J, Gulev S, Hanley J, Hewson T, Inatsu M, Keay K, Kew SF, Kindem I, Leckebusch GC, Liberato MLR, Lionello P, Mokhov II, Pinto JG, Raible CC, Reale M, Rudeva I, Schuster M, Simmonds I, Sinclair M, Sprenger M, Tilinina ND, Trigo IF, Ulbrich S, Ulbrich U, Wang XL, Wernli H (2013) IMILAST - a community effort to intercompare extratropical cyclone detection and tracking algorithms. Bulletin of the American Meteorological Society 94 (4): 529–547. doi 10.1175/BAMS-D-11-00154.1

Nieto R, Gimeno L, de la Torre L, Ribera P, Barriopedro D, García-Herrera R (2007) Interannual variability of cut-off low systems over the European sector: the role of blocking and the northern hemisphere circulation modes. Meteorology and Atmospheric Physics 96: 85-101. doi: http://dx.doi.org/10.1007/s00703-006-0222-7

Peñarrocha D, Estrela M, Millán M (2002) Classification of daily rainfall patterns in a Mediterranean area with extreme intensity levels: the Valencia region. International Journal of Climatology 22: 677–695. doi: 10.1002/joc.747

Perkins SE, Pitman AJ, Holbrook NJ, McAneney J (2007) Evaluation of the AR4 climate models' simulated daily maximum temperature, minimum temperature, and precipitation over Australia using probability density functions. Journal of Climate 20: 4356–4376. doi: 10.1175/JCLI4253.1

Pfahl S (2014) Characterising the relationship between weather extremes in Europe and synoptic circulation features. Natural Hazards and Earth System Sciences 14: 1461–1475. doi:10.5194/nhess-14-1461-2014

Rex DF (1950b) Blocking action in the middle troposphere and its effect upon regional climate. Part II: The climatology of blocking action. Tellus 2: 275–301.

Rex DF (1951) The effect of Atlantic blocking action upon European climate. Tellus 3: 1–16.

Ricard D, Ducrocq V, Auger L (2012) A Climatology of the Mesoscale Environment Associated with Heavily Precipitating Events over a Northwestern Mediterranean Area. Journal of Applied Meteorology and Climatology 51 (3): 468-488. doi: 10.1175/JAMC-D-11-017.1

Rolph GD (2003) Real-time Environmental Applications and Display sYstem (READY) Website (http://www.arl.noaa.gov/ready.php). NOAA Air Resources Laboratory, Silver Spring, MD.

Ruti PM, Dell'Aquila A, Giorgi F (2014) Understanding and attributing the Euro-Russian summer blocking signatures. Atmospheric Science Letters 15(3): 204-210. doi: 10.1002/asl2.490

Santos JA, Pinto JG, Ulbrich U (2009) On the development of strong ridge episodes over the eastern North Atlantic. Geophysical Research Letters 36: L17804. doi:10.1029/2009GL039086

760 Santos JA, Woollings T, Pinto JG (2013) Are the Winters 2010 and 2012 Archetypes Exhibiting Extreme
761 Opposite Behavior of the North Atlantic Jet Stream? Monthly Weather Review 131 (10): 3626-3640. doi:
762 10.1175/MWR-D-13-00024.1

763 Scaife AA, Woollings T, Knight J, Martin G, Hinton T (2010) Atmospheric Blocking and Mean Biases in
764 Climate Models. Journal of Climate 23: 6132-6152. doi: 10.1175/2010JCLI3728.1

765 Sillmann J and Croci-Maspoli M (2009) Present and future atmospheric blocking and its impact on
766 European mean and extreme climate. Geophysical Research Letters 36: L10702. doi:
767 10.1029/2009GL038259

768 Sillmann J, Croci-Maspoli M, Kallache M, Katz RW (2011) Extreme Cold Winter Temperatures in Europe
769 under the Influence of North Atlantic Atmospheric Blocking. Journal of Climate 24 (22): 5899-5913. doi:
770 10.1175/2011JCLI4075.1

771 Soares PMM, Cardoso RM, Ferreira JJ, Miranda PMA (2014) Climate change impact on Portuguese
772 precipitation: ENSEMBLES regional climate model results. Climate Dynamics 117: D07114. doi:
773 10.1007/s00382-014-2432-x

774 Sousa PM, Barriopedro D, Trigo RM, Ramos AM, Nieto R, Gimeno L, Turkman KF, Liberato MLR (2015)
775 Impact of Euro‐Atlantic blocking patterns in Iberia precipitation using a novel high resolution dataset.
776 Climate Dynamics. doi: 10.1007/s00382-015-2718-7

777 Treidl RA, Birch EC, Sajecki P (1981) Blocking action in the Northern Hemisphere: A climatological study.
778 Atmos.–Ocean 19: 1–23. doi: 10.1080/07055900.1981.9649096

779 Trigo IF (2006) Climatology and interannual variability of storm-tracks in the Euro-Atlantic sector: a
780 comparison between ERA-40 and NCEP/NCAR reanalyses. Climate Dynamics 26 (2-3): 127-143. doi:
781 10.1007/s00382-005-0065-9

782 Trigo RM, Trigo IF, DaCamara CC, Osborn TJ (2004) Winter blocking episodes in the European-Atlantic
783 sector: climate impacts and associated physical mechanisms in the reanalysis. Clim Dyn 23: 17–28. doi:
784 10.1007/s00382-004-0410-4

785 Trigo RM, Valente MA, Trigo IF, Miranda M, Ramos AM, Paredes D, García-Herrera R (2008) The Impact
786 of North Atlantic Wind and Cyclone Trends on European Precipitation and Significant Wave Height in the
787 Atlantic. Annals of the New York Academy of Sciences, 1146: 212-234. doi: 10.1196/annals.1446.014

788 Annals of the New York Academy of Sciences, 1146, 212-234, doi: 10.1196/annals.1446.014

789 Vial J and Osborn TJ (2012) Assessment of atmosphere-ocean general circulation model simulations of
790 winter Northern Hemisphere atmospheric blocking. Climate Dynamics 39: 95-112. doi: 10.1007/s00382-
791 011-1177-z)

792 Vicente-Serrano SM, Beguería S, Lopez-Moreno JI, El Kenawy AM, Angulo-Martinez M (2009) Daily
793 atmospheric circulation events and extreme precipitation risk in northeast Spain: Role of the North Atlantic
794 Oscillation, the Western Mediterranean Oscillation, and the Mediterranean. Journal of Geophysical
795 Research 114: D08106. doi:10.1029/2008JD011492

796 Vicente-Serrano SM, Trigo RM, López-Moreno JI, Liberato MLR, Lorenzo-Lacruz J, Beguería S, Morán-
797 Tejeda E, El Kenawy A (2011) Extreme winter precipitation in the Iberian Peninsula in 2010: anomalies,
798 driving mechanisms and future projections. Climate Research 46: 51-65. doi: 10.3354/cr00977

799 Wang L, Chen W, Zhou W, Chan JCL, Barriopedro D, Huang R (2010) Effect of the climate shift around
800 mid 1970's on the relationship between wintertime Ural blocking circulation and East Asian climate.
801 International Journal of Climatology 30 (1): 153-158. doi: 10.1002/joc.1876

802 Walter K and Graf HF (2005) The North Atlantic variability structure, storm tracks, and precipitation
803 depending on the polar vortex strength. Atmospheric Chemistry and Physics 5: 239-248.

804 Yao Y and Luo DH (2014a) Relationship between zonal position of the North Atlantic Oscillation and
805 Euro-Atlantic blocking events and its possible effect on the weather over Europe. Science China-Earth
806 Sciences 57 (11): 2626-2638. doi: 10.1007/s11430-014-4949-6

807 Yao Y and Luo DH (2014b) The Anomalous European Climates Linked to Different Euro-Atlantic
808 Blocking. Atmospheric and Oceanic Science Letters 7 (4): 309-313. doi: 10.3878/j.issn.1674-2834.14.0001

809

Fig.1- Thick black boxes identify the considered sectors for blocking center location: Atlantic (ATL) – from 30W to 0W; European (EUR) – from 0E to 30E; Russian (RUS) – from 30E to 60E. The shadings indicate the annual mean frequency of blocking center locations in each gridpoint. Blocks outside the 45N to 70N latitude strip were discarded in both sectors. Thin blue boxes identify areas which were considered in the regional assessment performed in Section 5.

Fig.2- Composites of the daily anomalies (shaded areas) and absolute values (isolines) of 500 hPa geopotential height for blocking centers in each sector and for all seasons. All values are in decameters (dam) and the thick line represents the 550 dam isohypse.

Fig.3- Annual composites for daily precipitation anomalies (%) in Europe during blocking (upper row) and strong zonal flow (middle row) days in the ATL (left column), EUR (central column) and RUS (right column) sectors. The difference between the regional blocking and strong zonal flow composites is presented in the bottom row. Only statistically significant anomalies at the 5% level are shown (two-sample Kolmogorov-Smirnov test).

Fig.4- Seasonal composites for the differences in absolute anomalies of daily precipitation (mm/day) between blocking and strong zonal flow patterns in the ATL (left column), EUR (central column) and RUS (right column) sectors. Only statistically significant anomalies at the 5% level are shown.

Fig.5- Top: Annual mean frequency of non-stationary cyclone centers (counted in 2.5ºx2.5º boxes). Middle row: annual mean changes (in %) in the cyclone frequency during blocking episodes in the ATL (middle left), EUR (middle center) and RUS (middle right) sectors. Bottom row: annual mean changes (in %) in the cyclone frequency during strong zonal flow episodes in the ATL (bottom left), EUR (bottom center) and RUS (bottom right) sectors. Increases are shown with blue shading and decreases with red shading. Stippling corresponds to areas with very low mean annual frequency of cyclone occurrence (below 0.5 per year).

Fig.6- Annual composites of the daily Integrated Vapour Transport (IVT, in kg m^{-1} s^{-1}, blue shading), and its anomaly in the bottom panels (red to green shading), the Lifted Index anomaly (LI, in C, reddish thick lines), 500hPa geopotential height (Z500, in dam, thin grey lines – the thicker grey line corresponds to the 550 dam isohypse) and mean horizontal transport (black arrows, kg m-1, s-1) for blocking (upper row) days, strong zonal flow days (middle row) days and their difference (bottom row). Left, center and right columns correspond to composites for weather patterns occurring in the ATL, EUR and RUS sectors, respectively.

Fig.7- Seasonal composites for the positive (negative) changes in the daily Integrated Vapor Transport (IVT, in kg m^{-1} s^{-1}) in green (brown) shading, the increment in atmospheric instability using the Lifted Index (LI, in C) in reddish thick lines, the positive (negative) changes in the 500hPa geopotential height (Z500, in dam) in solid (dashed) thin grey, when shifting from strong zonal flow to blocked patterns in the ATL (left column), EUR (central column) and RUS (right column) sectors. Arrows represent the mean horizontal transport of specific humidity.

852

853 Fig.8- Top: Annual mean latent heat flux (counted in 2.5ºx2.5º boxes). Middle row: annual mean changes
854 (in W/m^2) in the latent heat fluxes during blocking episodes in the ATL (middle left), EUR (middle center)
855 and RUS (middle right) sectors. Bottom row: annual mean changes (in W/m^2) in latent heat fluxes during
856 strong zonal flow episodes in the ATL (bottom left), EUR (bottom middle) and RUS (bottom right) sectors.
857 Increases are shown with blue shading (solid white lines) and decreases with red shading (dotted white
858 lines).

859

860 Fig.9- Shifts in the precipitation distribution of the UK during the different considered synoptic patterns.
861 Top: Relative frequency of days with precipitation totals, considering 1mm bins (grey bars) and the
862 corresponding contribution of each bin to the total annual precipitation (solid black line). Middle: Relative
863 change in the contribution of each bin to the total annual precipitation for blocked (solid lines) and zonal
864 (dashed lines) patterns in the three considered sectors (colored lines). Bottom: Cumulative change resulting
865 from the relative changes in the precipitation distribution associated to each blocked (solid lines) and zonal
866 (dashed lines) pattern. The thin vertical lines represent different percentiles of total daily precipitation
867 (considering only days above 1mm).

868

869 Fig.10- Same as Fig.9, but for the Iberian Peninsula.

870

871 Fig.11- Same as the previous, but for Russia, and considering only summer days.

872

873 Fig.12- Same as the previous, but for Turkey.

874

Figure

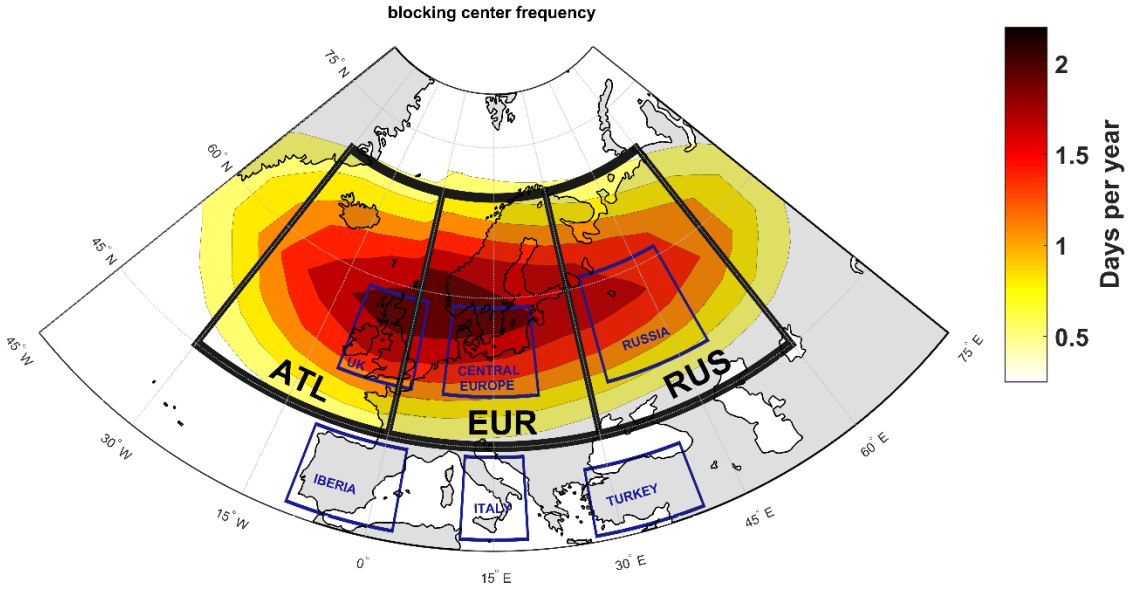

Fig.1- Thick black boxes identify the considered sectors for blocking center location: Atlantic (ATL) – from 30W to 0W; European (EUR) – from 0E to 30E; Russian (RUS) – from 30E to 60E. The shadings indicate the annual mean frequency of blocking center locations in each gridpoint. Blocks outside the 45N to 70N latitude strip were discarded in both sectors. Thin blue boxes identify areas which were considered in the regional assessment performed in Section 5.

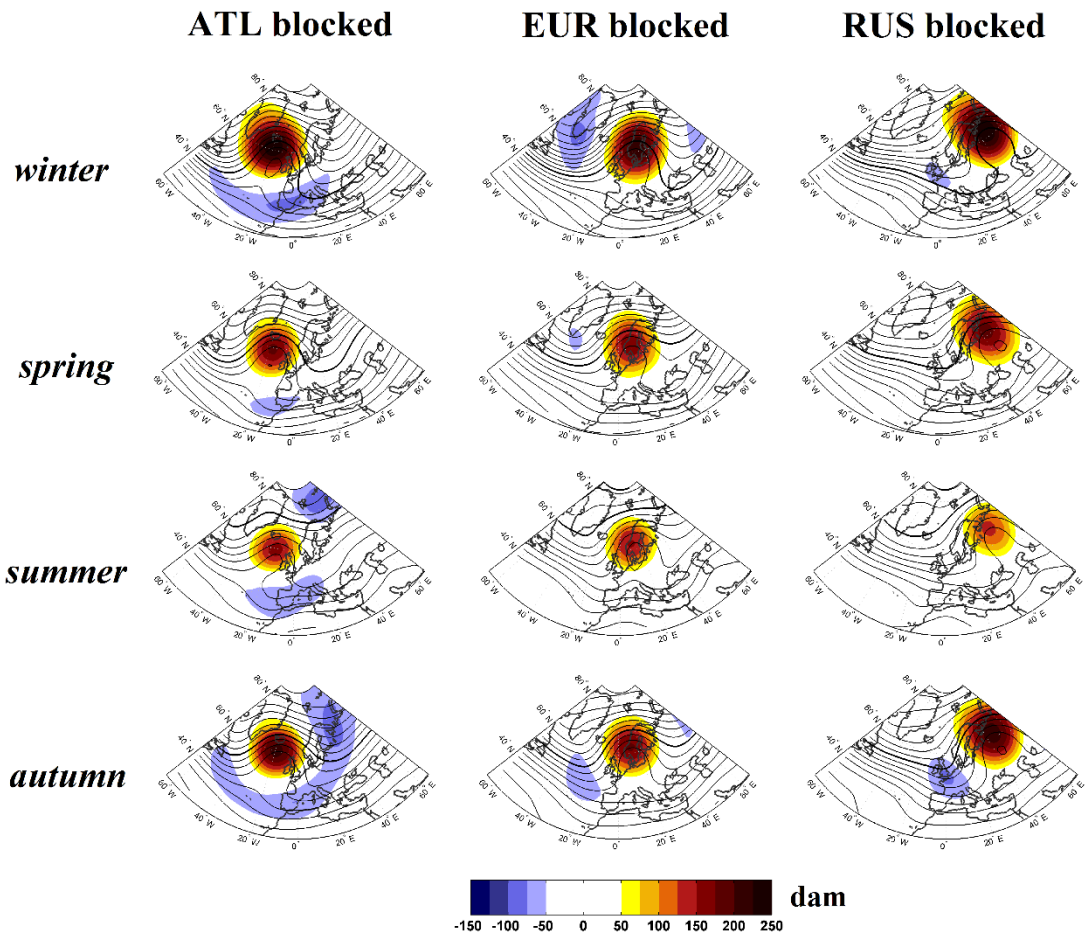

Fig.2- Composites of the daily anomalies (shaded areas) and absolute values (isolines) of 500 hPa geopotential height for blocking centers in each sector and for all seasons. All values are in decameters (dam) and the thick line represents the 550 dam isohypse.

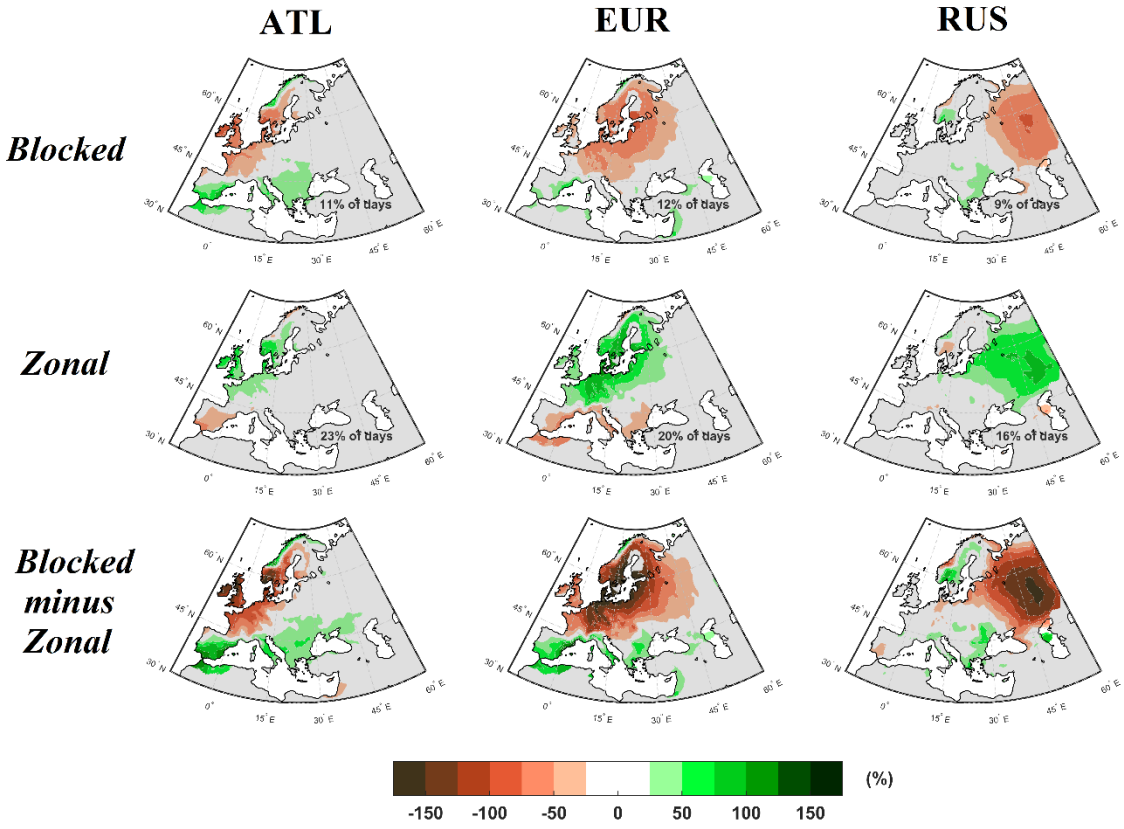

Fig.3- Annual composites for daily precipitation anomalies (%) in Europe during blocking (upper row) and strong zonal flow (middle row) days in the ATL (left column), EUR (central column) and RUS (right column) sectors. The difference between the regional blocking and strong zonal flow composites is presented in the bottom row. Only statistically significant anomalies at the 5% level are shown (two-sample Kolmogorov-Smirnov test).

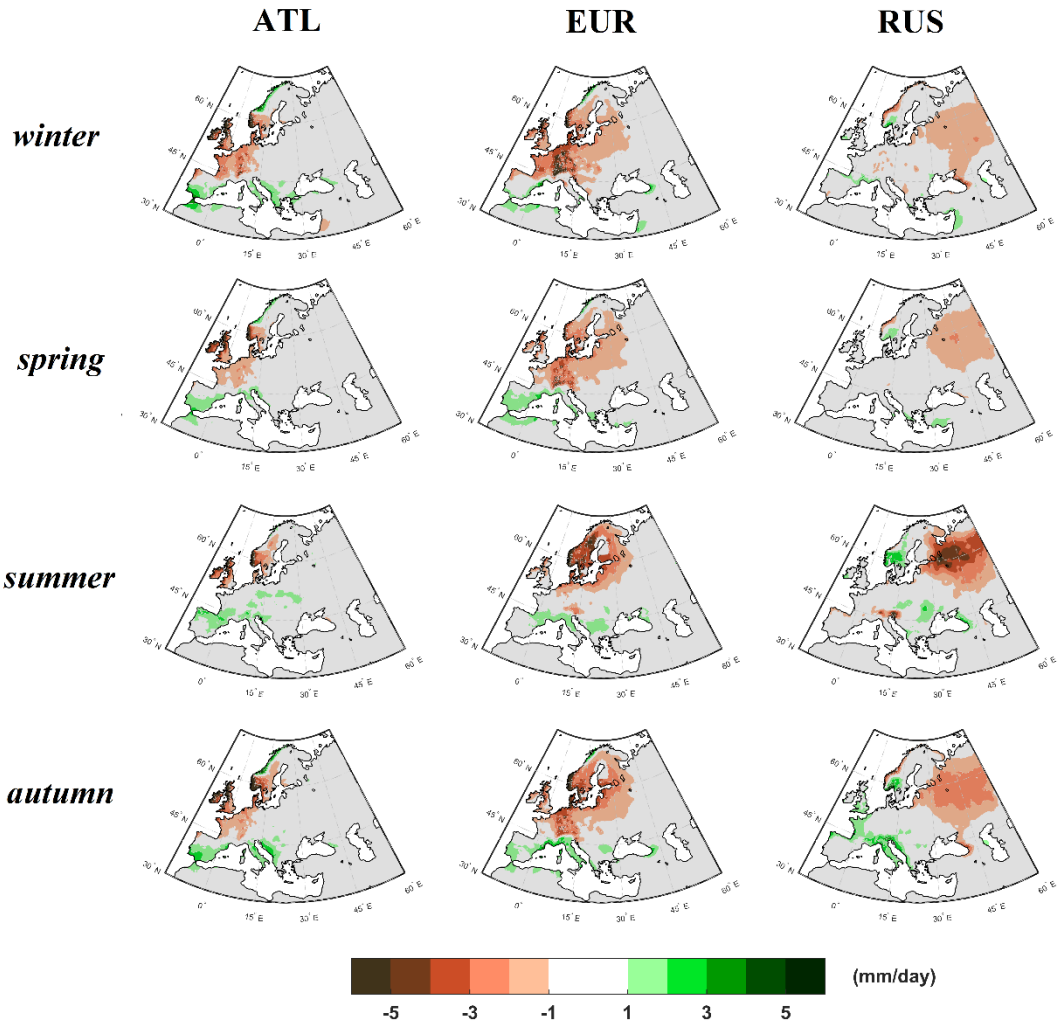

Fig.4- Seasonal composites for the differences in absolute anomalies of daily precipitation (mm/day) between blocking and strong zonal flow patterns in the ATL (left column), EUR (central column) and RUS (right column) sectors. Only statistically significant anomalies at the 5% level are shown.

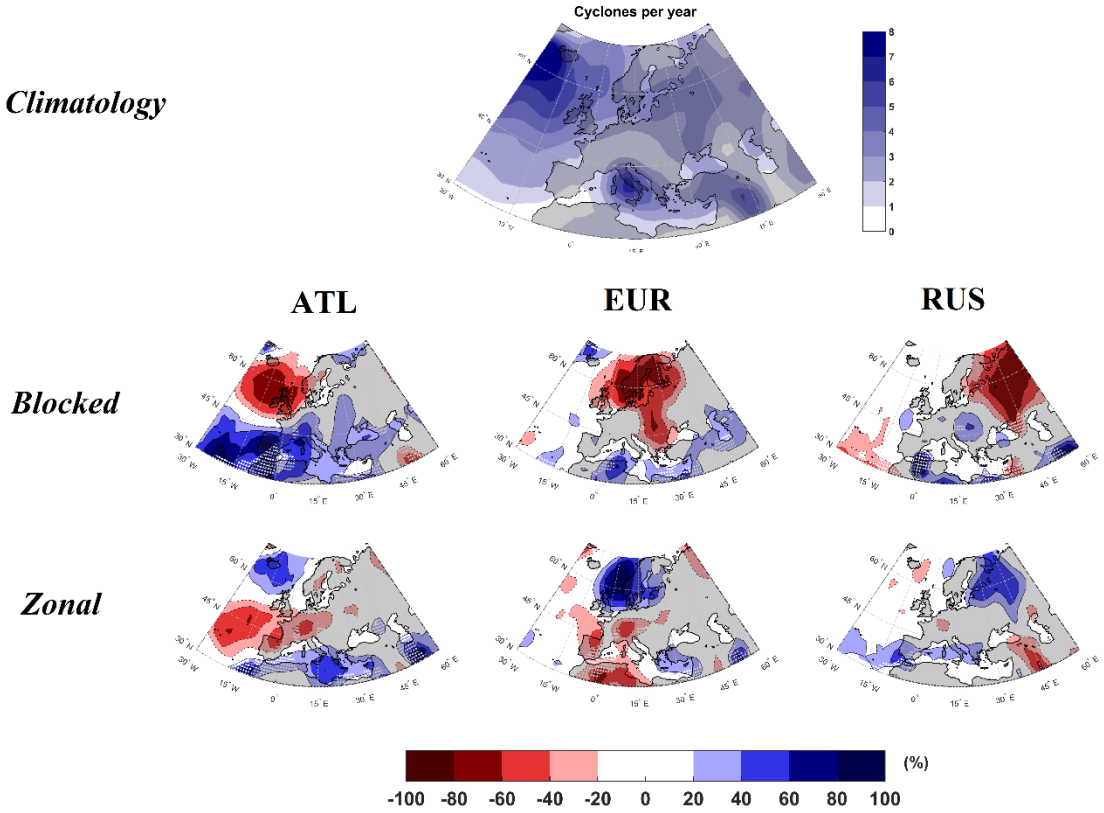

Fig.5- Top: Annual mean frequency of non-stationary cyclone centers (counted in 2.5ºx2.5º boxes). Middle row: annual mean changes (in %) in the cyclone frequency during blocking episodes in the ATL (middle left), EUR (middle center) and RUS (middle right) sectors. Bottom row: annual mean changes (in %) in the cyclone frequency during strong zonal flow episodes in the ATL (bottom left), EUR (bottom center) and RUS (bottom right) sectors. Increases are shown with blue shading and decreases with red shading. Stippling corresponds to areas with very low mean annual frequency of cyclone occurrence (below 0.5 per year).

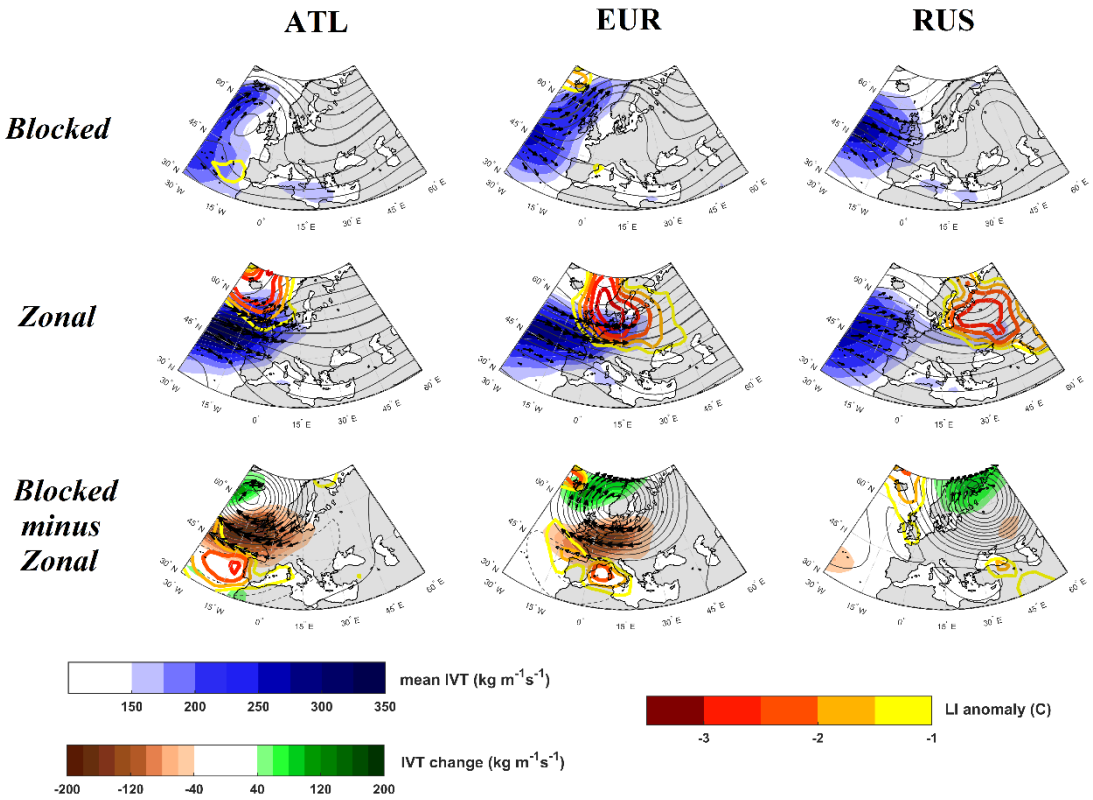

Fig.6- Annual composites of the daily Integrated Vapour Transport (IVT, in kg m^{-1} s^{-1}, blue shading), and its anomaly in the bottom panels (red to green shading), the Lifted Index anomaly (LI, in C, reddish thick lines), 500hPa geopotential height (Z500, in dam, thin grey lines – the thicker grey line corresponds to the 550 dam isohypse) and mean horizontal transport (black arrows, kg m-1, s-1) for blocking (upper row) days, strong zonal flow days (middle row) days and their difference (bottom row). Left, center and right columns correspond to composites for weather patterns occurring in the ATL, EUR and RUS sectors, respectively.

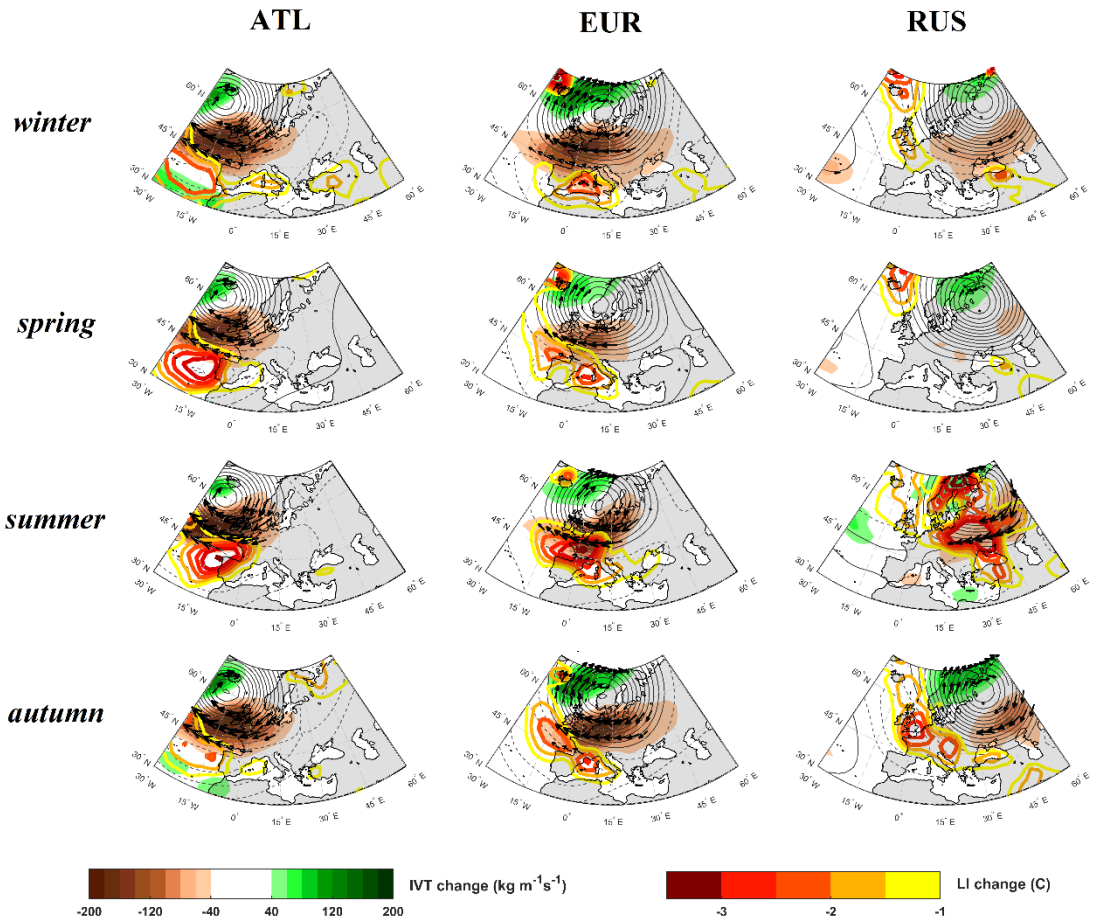

Fig.7- Seasonal composites for the positive (negative) changes in the daily Integrated Vapor Transport (IVT, in kg m^{-1} s^{-1}) in green (brown) shading, the increment in atmospheric instability using the Lifted Index (LI, in C) in reddish thick lines, the positive (negative) changes in the 500hPa geopotential height (Z500, in dam) in solid (dashed) thin grey, when shifting from strong zonal flow to blocked patterns in the ATL (left column), EUR (central column) and RUS (right column) sectors. Arrows represent the mean horizontal transport of specific humidity.

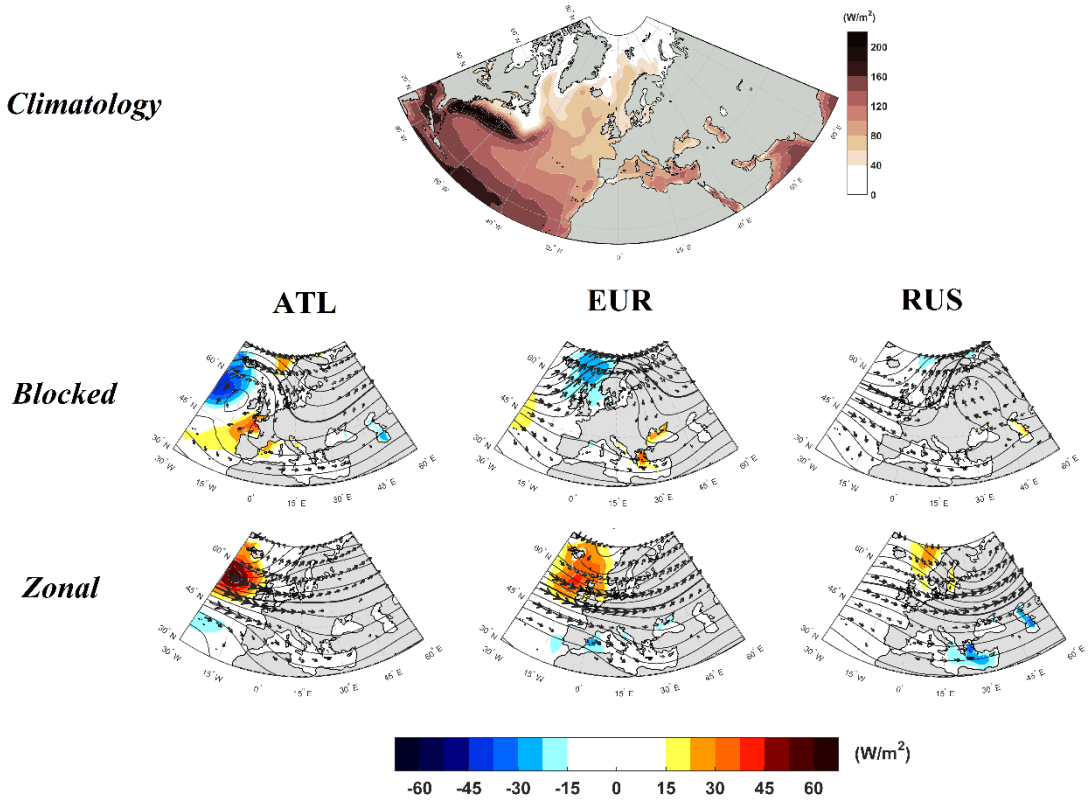

Fig.8- Top: Annual mean latent heat flux (counted in 2.5ºx2.5º boxes). Middle row: annual mean changes (in W/m^2) in the latent heat fluxes during blocking episodes in the ATL (middle left), EUR (middle center) and RUS (middle right) sectors. Bottom row: annual mean changes (in W/m^2) in latent heat fluxes during strong zonal flow episodes in the ATL (bottom left), EUR (bottom middle) and RUS (bottom right) sectors. Increases are shown with blue shading (solid white lines) and decreases with red shading (dotted white lines).

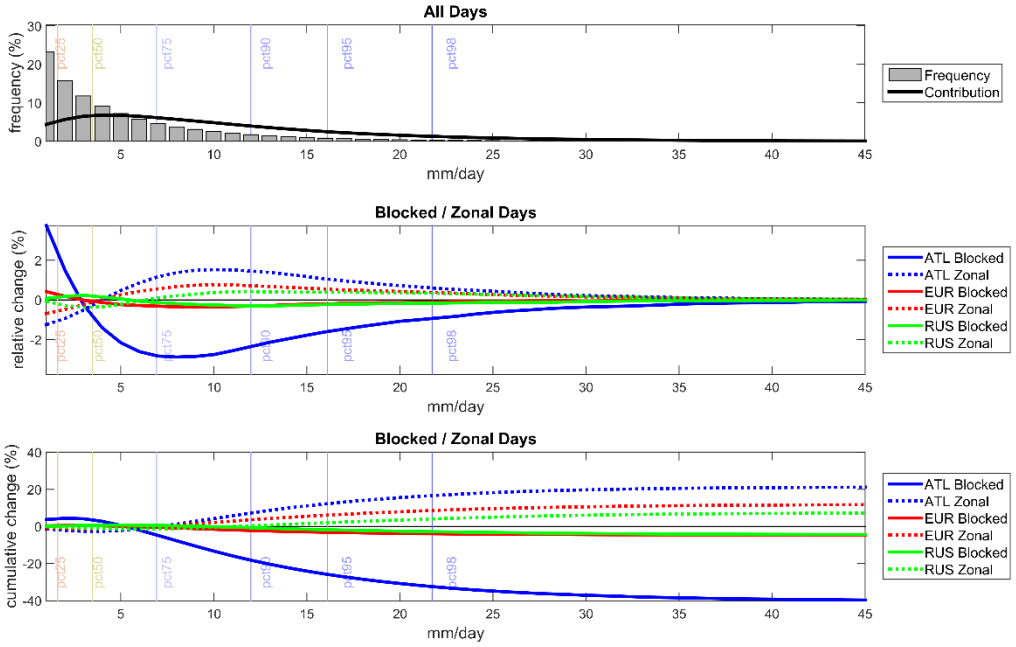

Fig.9- Shifts in the precipitation distribution of the UK during the different considered synoptic patterns. Top: Relative frequency of days with precipitation totals, considering 1mm bins (grey bars) and the

corresponding contribution of each bin to the total annual precipitation (solid black line). Middle: Relative change in the contribution of each bin to the total annual precipitation for blocked (solid lines) and zonal (dashed lines) patterns in the three considered sectors (colored lines). Bottom: Cumulative change resulting from the relative changes in the precipitation distribution associated to each blocked (solid lines) and zonal (dashed lines) pattern. The thin vertical lines represent different percentiles of total daily precipitation (considering only days above 1mm).

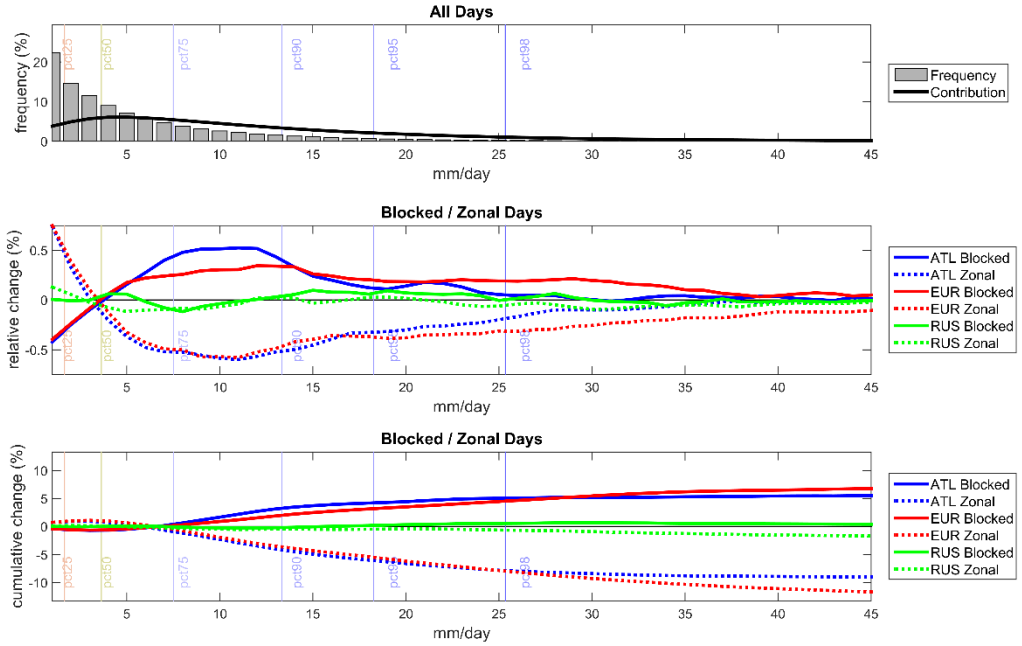

Fig.10- Same as Fig.9, but for the Iberian Peninsula.

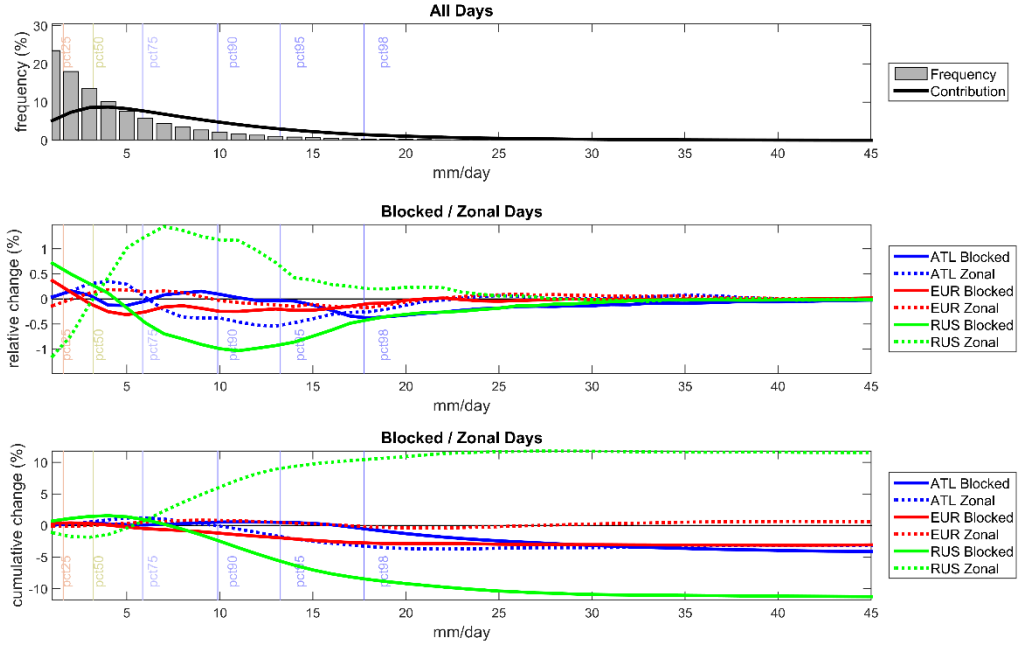

Fig.11- Same as the previous, but for Russia, and considering only summer days.

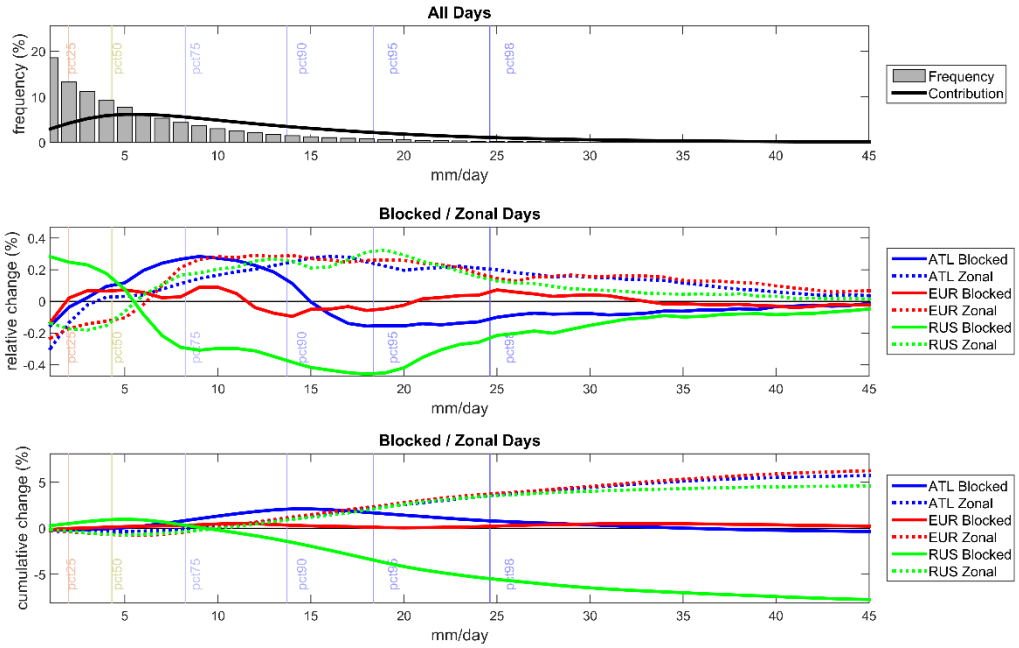

68

69 Fig.12- Same as the previous, but for Turkey.

70